Development 139, 2988-2998 (2012) doi:10.1242/dev.078675

The protein kinase MLTK regulates chondrogenesis by inducing the transcription factor Sox6

Toshiyasu Suzuki[1], Morioh Kusakabe[1,2], Kei Nakayama[1] and Eisuke Nishida[1,2,*]

SUMMARY

Sox9 acts together with Sox5 or Sox6 as a master regulator for chondrogenesis; however, the inter-relationship among these transcription factors remains unclear. Here, we show that the protein kinase MLTK plays an essential role in the onset of chondrogenesis through triggering the induction of Sox6 expression by Sox9. We find that knockdown of MLTK in *Xenopus* embryos results in drastic loss of craniofacial cartilages without defects in neural crest development. We also find that Sox6 is specifically induced during the onset of chondrogenesis, and that the Sox6 induction is inhibited by MLTK knockdown. Remarkably, Sox6 knockdown phenocopies MLTK knockdown. Moreover, we find that ectopic expression of MLTK induces Sox6 expression in a Sox9-dependent manner. Our data suggest that p38 and JNK pathways function downstream of MLTK during chondrogenesis. These results identify MLTK as a novel key regulator of chondrogenesis, and reveal its action mechanism in chondrocyte differentiation during embryonic development.

KEY WORDS: MLTK, Sox6, Sox9, Chondrocyte differentiation, *Xenopus*

INTRODUCTION

Neural crest cells, which are generated at the lateral edge of the neural plate, migrate extensively and differentiate into diverse derivatives, including much of the facial skeleton and peripheral nervous system. Neural crest cells are multipotent and give rise to various types of cells, including craniofacial cartilage, pigment cells, autonomic and enteric ganglia, neurons and smooth muscle cells (Sauka-Spengler and Bronner-Fraser, 2008). The neural crest can be divided into two main domains; cranial and trunk neural crest domains. Only the cells of cranial neural crest have a potential to generate chondrocytes and osteoblasts (Le Douarin et al., 2004). However, the mechanism of the differentiation of cranial neural crest cells into chondrocytes has not been well understood.

Sox5, Sox6 and Sox9 constitute a transcription factor trio that is essential for cartilage formation in mice (Lefebvre and Smits, 2005). Sox9 is expressed in multipotent mesenchymal cells (Ng et al., 1997; Zhao et al., 1997) and is required for cell survival and chondrocyte differentiation in cartilage primordia (Bi et al., 1999; Akiyama et al., 2002). Sox5 and Sox6, which are related to each other and functionally redundant in chondrogenesis, are expressed with Sox9 in pre-cartilaginous condensations and are essential for cartilage formation (Smits et al., 2001). Sox9 has a transactivation domain, but Sox5 and Sox6 do not (Lefebvre et al., 1998). Sox5 and Sox6 bind to the enhancers of cartilage matrix genes and enhance the activity of Sox9 (Han and Lefebvre, 2008; Nagy et al., 2011). The three Sox genes together are able to confer on non-chondrogenic cells the ability to activate *Col2a1*, *Agc1* and several other cartilage markers (Ikeda et al., 2004). Taken together, Sox5, Sox6 and Sox9 are not only required but also sufficient for chondrocyte differentiation. Although it has been reported that Sox9 induces *Sox5* and *Sox6* expression (Ikeda et al., 2004), neither the mechanism of this induction nor the inter-relationship among the three factors has been elucidated.

The mitogen-activated protein kinase (MAPK) pathways play an important role in transducing extracellular signals to the transcriptional program. The MAPK pathways consist of three sequentially activated protein kinases: MAPK kinase kinase (MAPKKK), MAPK kinase (MAPKK) and MAPK (Nishida and Gotoh, 1993; Robinson and Cobb, 1997; Chang and Karin, 2001). MLTKs (MLK-like mitogen-activated protein triple kinases) are a subfamily of the MLK family (Gallo and Johnson, 2002). Two splicing variants are identified in MLTKs that have identical amino acid sequences in the N-terminal region (residues 1-311), which contains a kinase domain and a leucine zipper motif. MLTKα has a longer C-terminal region containing a sterile-α-motif (SAM), which is absent from MLTKβ (Liu et al., 2000; Bloem et al., 2001; Gotoh et al., 2001). MLTKα and MLTKβ form homo- and heterodimers, and can be activated by osmotic stress (Liu et al., 2000; Gotoh et al., 2001). Activated MLTKα and MLTKβ activate the p38 and JNK pathways through MKK3/6 and MKK4/7 phosphorylation (Gotoh et al., 2001; Gross et al., 2002). In cultured cells, knockdown of MLTK completely blocks anisomycin- and UV-induced p38 and JNK activation and apoptosis (Wang et al., 2005). Transgenic mice with cardiac-restricted overexpression of MLTKβ have increased p38 pathway activation and characteristics of a cardiac compensatory phenotype (Christe et al., 2004). However, a role of MLTK in embryonic development remains unknown in any organism.

To study the function of MLTK in embryonic development, we isolated and knocked down MLTK in the *Xenopus* embryo. MLTK-depleted embryos showed severe defects in chondrocyte differentiation, while displaying normal neural crest formation and behavior. We also found that *Sox6*, but not *Sox5* or *Sox9*, is specifically induced during the onset of chondrogenesis, and the induction of Sox6 is required for chondrocyte differentiation. Importantly, our analysis demonstrated that MLTK plays a key role in inducing *Sox6* expression. These results identify MLTK as a key player in the differentiation of neural crest cells into chondrocytes.

[1]Department of Cell and Developmental Biology, Graduate School of Biostudies, Kyoto University, Sakyo-ku, Kyoto 606-8502, Japan. [2]JST, CREST, Chiyoda-ku, Tokyo 102-0075, Japan.

*Author for correspondence (nishida@lif.kyoto-u.ac.jp)

Accepted 1 June 2012

MATERIALS AND METHODS

Molecular cloning

A partial fragment (502 bp) of *Xenopus laevis MLTKβ* was obtained by PCR from stage 20 cDNA using a forward primer that was designed based on the *Xenopus tropicalis* EST sequence (GenBank Accession Number AL898835) homologous to mammalian *MLTKβ* (*B230120H23Rik* – Mouse Genome Informatics; *ZAK* – Human Gene Nomenclature Committee) and a reverse primer that was designed based on the sequence of mouse *MLTKβ* (Accession Number AB049732). A *Xenopus* gastrula stage cDNA library was then screened by plaque hybridization using this fragment as a probe, and the full-length clone of *xMLTKβ* was isolated. The entire coding region of *xMLTKα* was isolated by PCR from adult testis cDNA using a forward primer that was designed based on the N-terminal sequence of *xMLTKβ*, and a reverse primer that was designed based on the 3′ UTR sequence of *Xenopus tropicalis MLTKα* (XM_002934606). Partial fragments of *Xenopus laevis Agc1* and *Crtl1* were amplified by PCR from stage 46 cDNA using primers designed based on *Xenopus laevis* EST (EE317851), which contains a partial sequence of *xAgc1*, and *Xenopus tropicalis Crtl1* (XM_002933930), respectively. The coding regions of *Xenopus laevis Matn1* and *Sox5* were amplified by PCR from stage 18 and 48 cDNA using primers designed based on deposited sequences (*Matn1*, BC054272; *Sox5*, BC142559), respectively. As the obtained sequence of *xSox5* was different from the deposited sequence (BC142559), we submitted the obtained sequence and used this clone in our experiments. *Xenopus laevis Sox6*, including coding and untranslated regions, was amplified by PCR from stage 37/38 cDNA using primers designed based on *Xenopus tropicalis Sox6* (BC161247). Sequences of *xMLTKα*, *xMLTKβ*, *xCrtl1*, *xSox5* and *xSox6* have been deposited in GenBank under Accession Numbers AB682774, AB682773, AB682775, AB682776 and AB682777, respectively.

DNA constructs

To generate MO-resistant constructs for rescue experiments, eleven silent mutations were introduced into the MO target sequence of *xMLTKα* and *xMLTKβ* by site-directed mutagenesis, which substitutes ATGTTG-TCCTTAACGGCTTCGT with ATGTTAAGTCTTACTGCAAGTT (underlines indicate mutated nucleotides). The constitutively active form of *xMKK6* was constructed by replacing Ser208 and Thr212 of *xMKK6* (BC057716) with aspartic acid and glutamic acid, respectively. The constitutively active form of *xMKK7* was constructed as previously described (Yamanaka et al., 2002).

Immunoblotting

xMLTK-MO and mRNAs were injected into the animal pole of all blastomeres at the two-cell stage, and the embryos were harvested for lysis. Lysates were resolved by SDS-PAGE and subjected to immunoblotting according to a standard protocol. Mouse anti-Myc (9E10, Santa Cruz Biotechnology) or mouse anti-GFP (JL-8, Clontech) antibodies were used as a primary antibody, and sheep anti-mouse IgG HRP-conjugated (1:10,000; GE Healthcare) was used as a secondary antibody.

Embryo manipulation

Xenopus embryos were obtained by in vitro fertilization and cultured in 0.1× MBS at 22°C. Embryos were staged according to Nieuwkoop and Faber (Nieuwkoop and Faber, 1967). Antisense morpholino oligonucleotides (MOs), plasmid DNA and mRNA were injected into the animal pole of two or all blastomeres at the four-cell stage in 4% Ficoll in 0.1× MBS. In vitro synthesis of capped mRNA was performed using the mMESSAGE mMACHINE (Ambion). MOs were purchased from Gene Tools. The MO sequences were as follows: xMLTK-MO, 5′-ACGA-AGCCGTTAAGGACAACATCTC-3′; 5misMO, 5′-ACcAAGgCGTTA-AGcACAAgATgTC-3′ (lower case letters indicate mismatched bases); xSox9-MO, 5′-GCAAAAATGGGGAAAGGTAAGAAAG-3′ (Spokony et al., 2002); xSox5-MO, 5′-CTCGGGCTCAGTGAGCATTTCTG-3′; xSox6-MO, 5′-GCGGCTTGCTTGGAAGACATCCTTA-3′; and a standard control oligo (CoMO), 5′-CCTCTTACCTCAGTTACAAT-TTATA-3′. For qRT-PCR analysis, the heads of embryos were cut out at the level just posterior to gills using a scalpel.

Sandwich culture

Sandwich culture was performed according to the report by Furue et al. (Furue et al., 2002) with minor changes. mRNAs and/or MOs were injected into the animal pole at the one-cell stage. A presumptive ectodermal sheet (0.4 × 0.4 mm) was cut from the injected embryos at stage 9, and then it was treated with 100 ng/ml activin A in SS (1× Steinberg's solution containing 0.1% fatty acid-free BSA and 100 μg/ml kanamycin) for 1 hour. Then it was cultured in fresh SS without activin A for 1 hour. It was then sandwiched between two presumptive ectodermal sheets at stage 9 (0.8 mm × 0.8 mm), which were cut from the other injected embryos that had been cultured at 15°C to delay development. The sandwiched explants were cultured in SS in 96-well plates for 72 hours at 22°C.

Whole-mount in situ hybridization

Embryos were fixed in MEMFA [100 mM MOPS (pH 7.4), 2 mM EGTA, 1 mM $MgSO_4$, 3.7% formaldehyde] for 1-2 hours, dehydrated and stored in methanol. Whole-mount in situ hybridization was performed as described previously (Sive et al., 2000) using a robot (InSituPro, Intavis). DIG-labeled antisense RNA probes were synthesized from linearized plasmids encoding a partial or full-length cDNA sequence of *xFoxD3*, *xTwist*, *xSox9*, *xMatn1*, *xAgc1*, *xCrtl1*, *xSox5* and *xSox6*. The regions of cDNA used as templates are as follows: *xMLTKα* (AB682774), 1016-2382; *xMLTKβ* (AB682773), 1181-1502; *xFoxD3* (AB014611), coding region; *xTwist* (BC129769), coding region; *xSox9* (AY035397), coding region; *xMatn1* (BC054272), 1108-1518; *xAgc1* (EE317851), 109-641; *xCrtl1* (AB682775), 1-453; *xSox5* (AB682776), 1077-1623; *xSox6* (AB682777), 1172-1734.

Alcian Blue staining

Embryos were fixed in MEMFA for 1-2 hours, dehydrated and stored in methanol. Embryos were replaced with 100%, 75% and 50% ethanol, then stained overnight in the staining solution consisting of 0.01% Alcian Blue 8GX, 10% acetic acid and 60% ethanol.

Quantification of cartilage size

The length of ceratohyal cartilages was measured using the Photoshop measure tool. First, the distal tips of the right and left ceratohyal cartilages of each embryo were connected with a line. Second, the intersection between this line and the midline of the embryo was plotted to define the right and left parts of the line. Third, the lengths of the right and left parts of the line were measured. The relative cartilage size in Fig. 1F was calculated as the ratio of the length of the right part (injected side) to that of the left part (uninjected side) of the line.

Quantitative RT-PCR analysis

Total RNA was extracted from embryos using TRIzol reagent (Invitrogen), and cDNA was synthesized using reverse transcriptase M-MLV (Invitrogen) with random hexamer primers. Quantitative RT-PCR was performed on LightCycler (Roche Diagnostics) with QuantiTect SYBR Green PCR Kit (QIAGEN). The gene expression levels were normalized to those of *xODC* (ornithine decarboxylase). The sequences of primers used for qRT-PCR are as follows: *xMLTKα* (AB682774) (F, TCCGCTGATAAAGGATTTGG; R, CAGCTGCCTGATTTGAAGTG); *xMLTKβ* (AB682773) (F, GCCCTTGAAGAACAAGTCAAC; R, AGAAAGGCCACAGCAACAAG); *xMatn1* (BC054272) (F, AAGG-TCTTCCTGTCCCAGGT; R, AAGTGCTGGCTTTGCTTTGT); *xAgc1* (EE317851) (F, CCACGGGAGAAGATTGTGTT; R, CCACTGTTCC-CTTTTTGCAT); *xCrtl1* (AB682775) (F, GGTTCCGGGAGTACGA-AACT; R, GCAGGCTTGTACAGCTTCATC); *xSox5* (AB682776) (F, AGAGCTGCACATCAAGGAG; R, CAAAGTTCCCAGCTCTGGTC); *xSox6* (AB682777) (F, CGACGAGTGGAAGGAGGAC; R, CGTGAC-GCTAAATCCCCAGT); *xSox9* (AY035397) (F, TCCGTTAAGAAT-GGGCAGAC; R, CTCCAGGAGAGTGGACTTCG); *xODC* (BC044004) (F, TGCAAGTTGGAGACTGGATG; R, CATCAGTTGCCAGTGT-GGTC).

Microarray experiments

The injection procedure and embryo collection are described in the figure legend. Total RNA was extracted using TRIsol reagent, treated with DNase (TURBO DNase, Ambion) and then purified using RNeasy Mini Kit

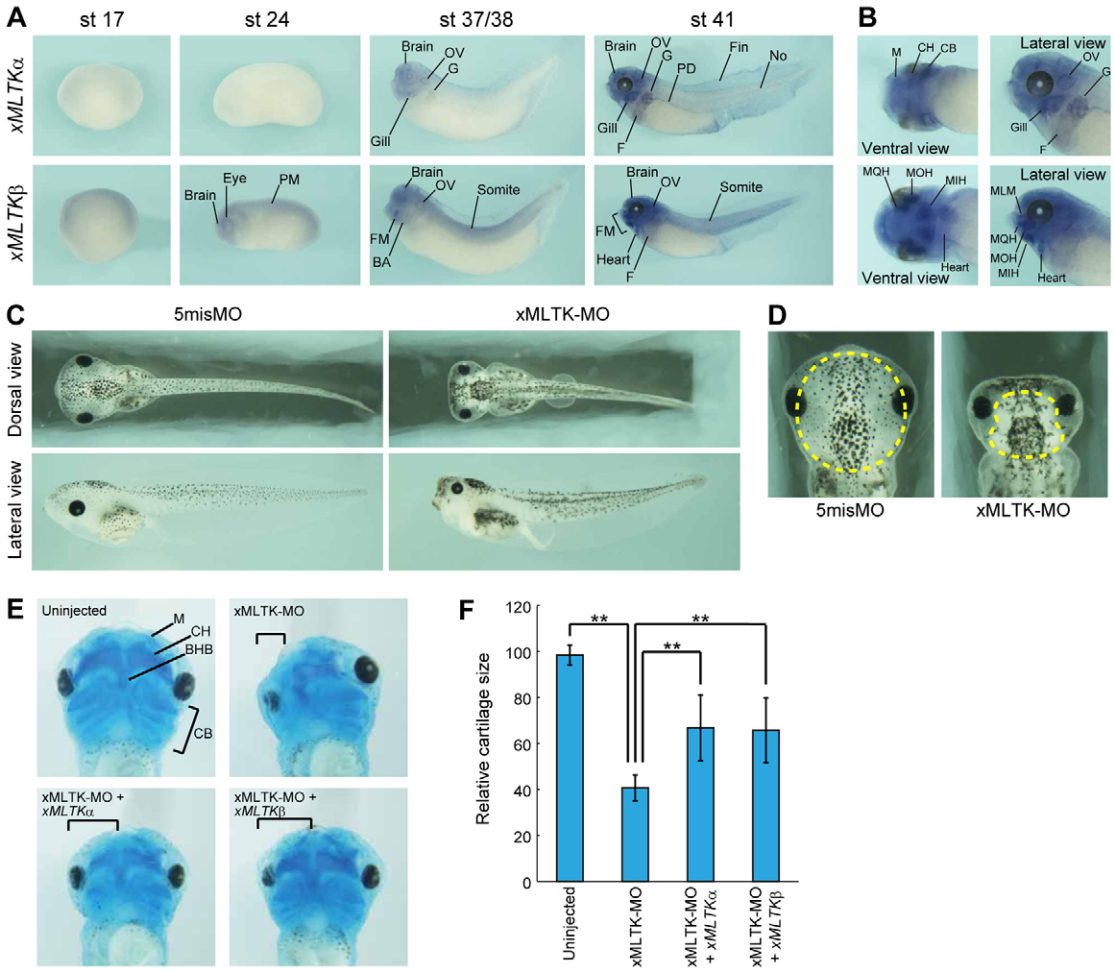

Fig. 1. xMLTK is required for craniofacial cartilage formation. (**A**) Whole-mount in situ hybridization for xMLTKα and xMLTKβ was performed on embryos at stages 17, 24, 37/38 and 41. OV, otic vesicle; G, glomus; PD, pronephric duct; No, notochord; F, left-rostral furrow in yolk mass; PM, paraxial mesoderm; FM, facial muscle; BA, branchial arch. (**B**) Magnified view of embryos at stage 41 shown in A. M, Meckel's cartilage; CH, ceratohyal cartilage; CB, ceratobranchial cartilage; OV, otic vesicle; G, glomus; F, left-rostral furrow in yolk mass; MQH, m. quadrato-hyoangularis; MOH, m. orbitohyoideus; MIH, m. interhyoideus; MLM, m. levator mandibulae. (**C**) xMLTK-MO or 5misMO was injected into the animal pole of all blastomeres (10 ng/cell) at the four-cell stage, and the embryos were fixed at stage 45. (**D**) Magnified view of the head of the embryo shown in C. Craniofacial cartilage is outlined with a dashed yellow line. (**E**) xMLTK-MO (*n*=29), xMLTK-MO plus xMLTKα-res-myc plasmid (n=25), or xMLTK-MO plus xMLTKβ-res-myc plasmid (*n*=25) was injected unilaterally into the animal pole of two blastomeres (xMLTK-MO, 10 ng/cell; plasmid, 50 pg /cell) at the four-cell stage. Uninjected embryos (n=31) and injected embryos were fixed at stage 45, and cartilages were stained with Alcian Blue. Brackets indicate the injected side. M, Meckel's cartilage; CH, ceratohyal cartilage; CB, ceratobranchial cartilage; BHB, basihyobranchial cartilage. (**F**) The relative cartilage size (the rate of the length of the right side to that of the left side of ceratohyal cartilages) was quantified. Values are mean±s.d. $^{**}P<0.01$.

(QIAGEN) according to the manufacturer's instructions. The quality of total RNA was assessed using the Agilent 2100 BioAnalyzer. Reverse transcription to synthesize first-strand cDNA, second-strand cDNA synthesis, in vitro transcription to synthesize Biotin-modified aRNA, aRNA purification and fragmentation of the labeled aRNA were performed using the GeneChip 3′ IVT Express Kit and hybridization to the Affymetrix GeneChip *Xenopus laevis* Genome 2.0 Array was performed using the GeneChip Hybridization Wash and Stain Kit according to the manufacturer's instructions.

Microarray data analysis

Raw data (CEL files) were imported into Expression Console software for statistical analysis and GeneSpring GX 11.5.1 software for presentation of the scatter plots, clustering analysis and expression profiles. Signal intensities were normalized using RMA algorithm. Clustering analysis was performed with the following algorithm: clustering algorithm, hierarchical; distance metric, chebyshev; linkage rule, complete. Because many of probe sets in Affymetrix GeneChip *Xenopus laevis* Genome 2.0 Array have no information on gene titles and symbols, the target sequences of *Xenopus laevis* probe sets were aligned to mouse reference sequences to obtain information on mouse orthologs to genes that are targeted by *Xenopus laevis* probe sets. First, all target sequences of probe sets were subjected to a BLASTN search against the all species RefSeq nucleotide database (NCBI version, as of September 7, 2010) with a maximum E value of 2.0×10^{-4}. Next, the top hit sequences were subjected to a BLASTX search against the mouse RefSeq protein database (NCBI version, as of September 7, 2010) with a maximum E value of 1.0×10^{-5}. The obtained mouse gene symbols, together with signal intensity from our microarray data, were then subjected to gene set enrichment analysis (Subramanian et al., 2005). The microarray data have been deposited in the National Center for Biotechnology Information (NCBI) Gene Expression Omnibus (GEO) with series accession number GSE33767.

Statistical analysis

Statistical differences were assessed with the unpaired Student's *t*-test. Data are presented as mean±s.d., and *P* values less than 0.05 were considered to be statistically significant.

RESULTS

Isolation and expression of Xenopus MLTKα and MLTK β

We isolated genes encoding *Xenopus laevis MLTKα* (*xMLTKα*) and *MLTKβ* (*xMLTKβ*). xMLTKα and xMLTKβ consist of 793 and 438 amino acids, respectively. Like human MLTKs, xMLTKα and xMLTKβ have the identical amino acid sequence in the N-terminal region (residues 1-330), which contains a kinase domain (16-277) and a leucine zipper motif (287-322). xMLTKα has a longer C-terminal region containing a sterile-α-motif (SAM) (339-406) (supplementary material Fig. S1A). At the amino acid level, xMLTKα and xMLTKβ shared 68% and 86% identity with human MLTKα and MLTKβ (NP_057737 and NP_598407), respectively. MLTKs are highly conserved in vertebrates (supplementary material Fig. S1B).

Quantitative RT-PCR (qRT-PCR) analysis at different stages of development showed that *xMLTKα* and *xMLTKβ* were expressed maternally, and their expression levels were decreased at the gastrula and neurula stages (stages 11-19). Increased expressions were detected at the early tailbud stage and persisted through the tadpole stage (supplementary material Fig. S2A). We next performed whole-mount in situ hybridization (Fig. 1A,B and supplementary material Fig. S2B). At stages 37/38 and 41, *xMLTKα* expression was detected in various tissues including the head, gill, pronephron and others. *xMLTKβ* was expressed in the neural tissues and paraxial mesoderm at stages 17, 24 and 37/38. Histological section showed that *xMLTKβ* was also expressed in the presumptive epidermis (supplementary material Fig. S2C). At stage 41, *xMLTKβ* expression was increased in the head, heart and left-rostral furrow in yolk mass (Fig. 1A,B).

xMLTK is required for craniofacial cartilage formation

To investigate the function of xMLTK during embryonic development, we performed knockdown of xMLTK by morpholino antisense oligonucleotides (MOs). An xMLTK-MO was designed to interfere with translation of both *xMLTKα* and *xMLTKβ* mRNAs. Immunoblotting analysis confirmed that xMLTK-MO blocked xMLTK protein production in a dose-dependent manner (supplementary material Fig. S3A). We next injected xMLTK-MO into the animal pole of all blastomeres of four-cell stage embryos. Although the injected embryos appeared normal until stage 35/36, they exhibited several defects at stage 45, including edema formation, body axis bending, small eyes and a drastic reduction of craniofacial cartilage (Fig. 1C,D). Injection of a five-base mismatched MO (5misMO) at the same dose had little or no effect on embryonic development (Fig. 1C,D). Alcian Blue staining revealed that all cartilaginous elements, especially Meckel's and quadrate cartilage, were drastically reduced on the injected side of the embryos unilaterally injected with xMLTK-MO (Fig. 1E, upper right panel).

To further assess the specificity of xMLTK-MO, we next asked whether the reduction of craniofacial cartilages in xMLTK-MO injected embryos could be rescued by expressing *xMLTKα* or *xMLTKβ*. In rescue experiments, we used *xMLTKα*-res-myc and *xMLTKβ*-res-myc, which carried an 11 bp mutation within the target sequence of xMLTK-MO and had a myc tag at the C terminus. Immunoblotting analysis confirmed that xMLTK-MO failed to block translation of *xMLTKα*-res-myc and *xMLTKβ*-res-myc mRNAs (supplementary material Fig. S3B). We unilaterally injected xMLTK-MO with or without *xMLTKα*-res-myc or *xMLTKβ*-res-myc plasmid into the animal pole of two blastomeres of four-cell stage embryos, and compared the length of ceratohyal cartilage between the injected and uninjected sides of each embryo. Co-injection of *xMLTKα*-res-myc or *xMLTKβ*-res-myc plasmid with xMLTK-MO significantly restored the size of cartilage when compared with siblings that received injection of xMLTK-MO alone (Fig. 1E,F). Collectively, these results show that xMLTK is required for craniofacial cartilage formation in *Xenopus*.

xMLTK is dispensable for neural crest formation and migration but required for chondrocyte differentiation

Craniofacial cartilage is mostly derived from neural crest cells, which pass through two fundamental steps: the formation and migration steps. We next examined whether xMLTK depletion disturbed neural crest formation and migration. Injection of xMLTK-MO did not substantially affect the expression levels and patterns of an early neural crest marker *xFoxD3* (Pohl and Knöchel, 2001; Sasai et al., 2001) (Fig. 2A), a migrating neural crest marker *xTwist* (Hopwood et al., 1989) (Fig. 2B) and a cranial neural crest marker *xSox9* (Spokony et al., 2002; Kerney et al., 2007) at stage 35/36, when neural crest cells reside in the branchial arches after migration (Fig. 2C). These results indicate that all steps of neural crest development are normal in xMLTK-depleted embryos.

We then examined whether xMLTK depletion affected chondrocyte differentiation. So far, few chondrocyte markers had been characterized in *Xenopus*. Therefore, we isolated the *Xenopus laevis* orthologs of matrilin 1 (*Matn1*), aggrecan (*Agc1*) and cartilage link protein 1 (*Crtl1*), which are known as chondrocyte markers (Lefebvre and Smits, 2005). Whole-mount in situ hybridization analysis showed that their expressions were detected in the prospective ceratohyal cartilage at stage 39, and increased strongly in all cartilaginous elements at stage 41 (supplementary material Fig. S4A-C). However, *xSox9* was expressed at stage 35/36 in the branchial arch and also in cartilages at stage 41 (Kerney et al., 2007) (supplementary material Fig. S4D). These results demonstrated that *xMatn1*, *xAgc1* and *xCrtl1* could be used as chondrocyte markers in *Xenopus*. qRT-PCR analysis also revealed that the expression levels of these three chondrocyte markers began to increase at around 60 hours after fertilization (corresponding to stage 39) (control lines in Fig. 2D). These results indicate that chondrocyte differentiation occurs around stage 39 in *Xenopus*.

We next analyzed their expression in xMLTK-depleted embryos by qRT-PCR. The heads of xMLTK-MO-injected embryos were collected in order to minimize contamination from other tissues than cartilages. The rise in the expression levels of *xMatn1*, *xAgc1* and *xCrtl1* was strongly suppressed in xMLTK-depleted embryos (Fig. 2D). Whole-mount in situ hybridization for chondrocyte markers showed that their expression levels in the cartilaginous skeletal elements, including the Meckel's, ceratohyal and ceratobranchial cartilages, were markedly reduced on the xMLTK-MO-injected side (Fig. 2E). Injection of a standard control MO (CoMO) or 5misMO did not reduce their expression levels (supplementary material Fig. S5A-C). These results taken together demonstrate that chondrocyte differentiation is inhibited by xMLTK knockdown, and thus indicate that xMLTK is required for chondrocyte differentiation, which starts around stage 39.

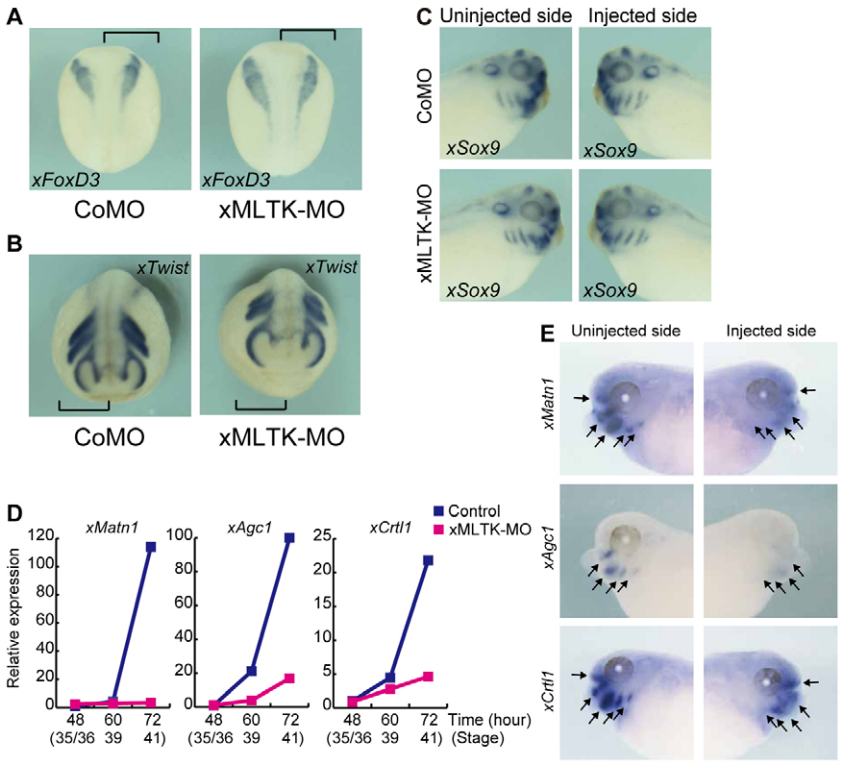

Fig. 2. xMLTK is required for chondrocyte differentiation but not for neural crest development. (**A-C**) xMLTK-MO or CoMO was injected unilaterally into the animal pole of two blastomeres (10 ng/cell) at the four-cell stage, and the embryos were fixed at stages 17 (A), 19 (B) and 35/36 (C). Whole-mount in situ hybridization was performed with xFoxD3 (A), xTwist (B) and xSox9 (C) probes. Brackets indicate the injected side. Frequency of specimen with the indicated phenotype (nearly equal expression) was CoMO in A, 11/11; xMLTK-MO in A, 17/19; CoMO in B, 5/6; xMLTK-MO in B, 15/15; CoMO in C, 13/13; xMLTK-MO in C, 10/12. (**D**) xMLTK-MO was injected into the animal pole of all blastomeres (10 ng/cell) at the four-cell stage. The heads of uninjected and injected embryos were cut out and harvested at 48, 60 and 72 hours after fertilization (corresponding to stages 35/36, 39 and 41, respectively). The expression levels of chondrocyte markers xMatn1, xAgc1 and xCrtl1 were analyzed by qRT-PCR. Representative results from two independent experiments are shown. (**E**) xMLTK-MO was injected unilaterally into the animal pole of two blastomeres (10 ng/cell) at the four-cell stage, and the embryos were fixed at stage 41. Whole-mount in situ hybridization was performed with xMatn1, xAgc1 and xCrtl1 probes. Arrows indicate presumptive cartilaginous elements. Frequency of specimen with the indicated phenotype (markedly reduced expression) was xMatn1, 19/21; xAgc1, 20/20; xCrtl1, 17/19.

xMLTK is required for xSox6 expression

In mice, Sox5, Sox6 and Sox9 play a pivotal role in chondrogenesis. So, we analyzed the expression of their *Xenopus* orthologs before and after chondrocyte differentiation. qRT-PCR analysis showed that although the expression levels of *xSox5* and *xSox9* were not changed substantially during this period, *xSox6* expression was increased markedly in the heads of embryos (Fig. 3A, blue bars). Interestingly, the increase in *xSox6* expression was suppressed in xMLTK-depleted embryos (Fig. 3A). It should be also noted that the expression levels of *xSox5* and *xSox9* were not substantially decreased by xMLTK knockdown (Fig. 3A). Time-course measurements of *xSox6* expression confirmed the marked upregulation of *xSox6* during the onset of chondrocyte differentiation and its suppression by xMLTK knockdown (Fig. 3B). Whole-mount in situ hybridization also showed that the increased *xSox6* expression in the head region at stage 41 (around 60 hours after fertilization) was dramatically reduced in the xMLTK-knockdown embryos (Fig. 3C). These results indicate that xMLTK is required for xSox6 expression.

We then inquired whether xMLTK is able to induce *xSox6* expression. Overexpression of *xMLTKα* and *xMLTKβ* by injecting their mRNAs in *Xenopus* embryos, however, did not induce *xSox6* expression (Fig. 3D). Therefore, we considered the possibility that xMLTK could collaborate with xSox9 to induce *xSox6* expression, as Sox9 can induce *Sox6* expression in mammalian cultured cells (Ikeda et al., 2004). As expected, although overexpression of *xSox9* alone did not induce a substantial increase in *xSox6* expression, co-expression of *xMLTKα* and *xMLTKβ* with *xSox9* induced marked increases in *xSox6* expression in a dose-dependent manner (Fig. 3E). Moreover, we examined whether the induction of *xSox6* expression by xMLTK requires xSox9 and vice versa. For longer culture, we employed a sandwich-culture method of craniofacial cartilage induction in vitro (Furue et al., 2002) (Fig. 3F). Although injection of *xMLTKα* and *xMLTKβ* mRNAs increased *xSox6* expression in 3-day sandwiched explants, co-injection of xSox9-MO markedly decreased *xSox6* expression (Fig. 3G). Whereas injection of *xSox9* mRNA increased *xSox6* expression, co-injection of xMLTK-MO substantially decreased *xSox6* expression (Fig. 3H). These results indicate that xMLTK functions to induce *xSox6* expression during chondrocyte differentiation through xSox9.

xSox6 is essential for craniofacial cartilage formation

Is the increased *xSox6* expression essential for craniofacial cartilage formation? In *Xenopus*, although xSox9 has been studied extensively (Spokony et al., 2002; Lee and Saint-Jeannet, 2011), the roles of xSox5 and xSox6 during embryonic development have not been studied. First, we analyzed the expression patterns of *xSox5*. Whole-mount in situ hybridization analysis confirmed the previously published expression patterns of *xSox5* from stage 26 to 41 (Martin and Harland, 2001) and also showed that *xSox5* was expressed at stage 15 in the anterior neural fold, paraxial mesoderm and neural crest (supplementary material Fig. S6A-D). We then isolated *xSox6* (supplementary material Fig. S6A) and analyzed its expression. In contrast to *xSox5*, *xSox6* expression at stages 15 to 23 was very low (supplementary material Fig. S6B) and undetectable by in situ hybridization (Fig. 4A). *xSox6* expression was first detected in the otic vesicle, somite and branchial arch at stage 29/30, and in the brain and posterior notochord at stage 35/36. At stage 39, when mesenchymal cells begin to differentiate into chondrocytes, *xSox6* expression in the branchial arches was dramatically increased, and each cartilaginous element was clearly distinguishable (Fig. 4A,B).

We then knocked down xSox5 and xSox6 by using xSox5-MO and xSox6-MO, respectively. Injection of xSox5-MO resulted in a modest reduction of craniofacial cartilage at stage 45 (supplementary material Fig. S7A,B). Conversely, injection of the

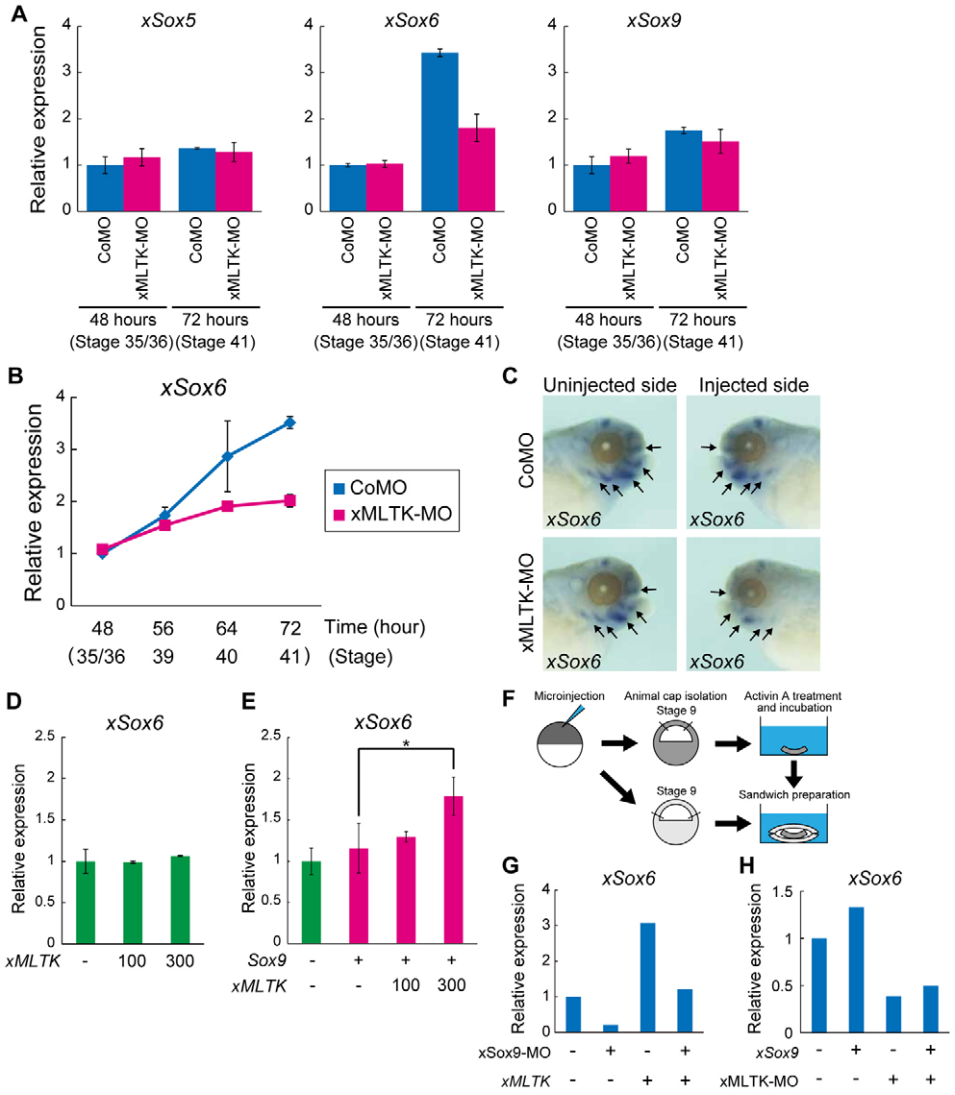

Fig. 3. xMLTK is required for xSox6 expression. (**A**) xMLTK-MO or CoMO was injected into the animal pole of all blastomeres (10 ng/cell) at the four-cell stage. The heads of embryos were cut out and harvested 48 and 72 hours after fertilization (corresponding to stages 35/36 and 41, respectively). The expression levels of xSox5, xSox6 and xSox9 were analyzed by qRT-PCR. Values are mean±s.d. of three independent experiments. (**B**) xMLTK-MO or CoMO was injected into the animal pole of all blastomeres (10 ng/cell) at the four-cell stage. The heads of embryos were cut out and harvested 48, 56, 64 and 72 hours after fertilization (corresponding to stages 35/36, 39, 40 and 41, respectively). The expression level of xSox6 was analyzed by qRT-PCR. Values are means ±s.d. of two independent experiments. (**C**) xMLTK-MO or CoMO was injected unilaterally into the animal pole of two blastomeres (10 ng/cell) at the four-cell stage, and the embryos were fixed at stage 41. Whole-mount in situ hybridization was performed with xSox6 probe. Arrows indicate presumptive cartilaginous elements. Frequency of specimen with the indicated phenotype (nearly equal expression in CoMO-injected embryos; markedly reduced expression in xMLTK-MO-injected embryos) was CoMO, 24/24; xMLTK-MO, 50/63. (**D**) xMLTKα-myc and xMLTKβ-myc mRNAs (50 or 150 pg of each/embryo) were injected into the animal region of two ventral blastomeres at the four-cell stage, and the embryos were harvested at stage 10.5. The expression level of xSox6 was analyzed by qRT-PCR. Values are mean±s.d. of two independent experiments. (**E**) HA-xSox9 mRNA (150 pg/embryo) was co-injected with or without both xMLTKα-myc and xMLTKβ-myc mRNAs (50 or 150 pg of each/embryo) into the animal region of two ventral blastomeres at the four-cell stage, and the embryos were harvested at stage 10.5. The expression level of xSox6 was analyzed by qRT-PCR. Values are mean±s.d. of three independent experiments. *P<0.05. (**F**) Schematic of sandwich culture experiments. (**G**) xMLTKα and xMLTKβ mRNAs (150 pg of each/embryo) and/or xSox9-MO (5 ng/embryo) were injected at the one-cell stage, and the embryos were used for sandwich culture experiments. Sandwiched explants were cultured for 72 hours and the expression level of xSox6 was analyzed by qRT-PCR. Representative results from two independent experiments are shown. (**H**) xSox9 mRNA (150 pg/embryo) and/or xMLTK-MO (40 ng/embryo) were injected at the one-cell stage, and the embryos were used for sandwich culture experiments. Sandwiched explants were cultured for 72 hours and the expression level of xSox6 was analyzed by qRT-PCR. Representative results from two independent experiments are shown.

same dose of xSox6-MO resulted in a drastic reduction of craniofacial cartilage (Fig. 4C and supplementary material Fig. S7B). Moreover, Alcian Blue staining showed that all cartilaginous elements in the head region were drastically reduced by xSox6-MO injection (Fig. 4D). These results suggest that xSox6 plays an essential role in craniofacial cartilage formation, and thus the increase in xSox6 expression at the onset of chondrocyte differentiation may be a key step in triggering chondrogenesis.

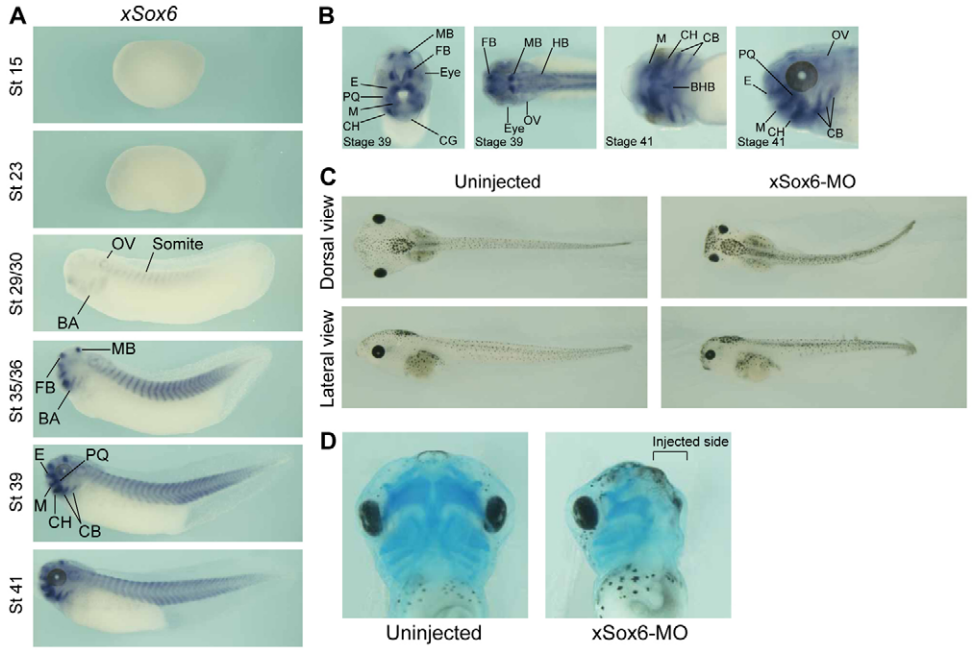

Fig. 4. xSox6 is required for craniofacial cartilage formation. (**A**) Whole-mount in situ hybridization for xSox6 was performed on embryos at stages 15, 23, 29/30, 35/36, 39 and 41. OV, otic vesicle; BA, branchial arch; FB, forebrain; MB, midbrain; E, ethmoid cartilage; PQ, palatoquadrate cartilage; M, Meckel's cartilage; CH, ceratohyal cartilage; CB, ceratobranchial cartilage. (**B**) Magnified view of the head of embryos shown in A. FB, forebrain; MB, midbrain; HB, hindbrain; OV, otic vesicle; CG, cement gland; E, ethmoid cartilage; PQ, palatoquadrate cartilage; M, Meckel's cartilage; CH, ceratohyal cartilage; CB, ceratobranchial cartilage; BHB, basihyobranchial cartilage. (**C**) xSox6-MO was injected into the animal pole of all blastomeres (10 ng/cell) at the four-cell stage, and the embryos were fixed at stage 45. (**D**) xSox6-MO was injected unilaterally into the animal pole of two blastomeres (10 ng/cell) at the four-cell stage. Uninjected and injected embryos were fixed at stage 45, and cartilages were stained with Alcian Blue.

xSox6 is required for chondrocyte differentiation but dispensable for neural crest formation and migration

To further characterize the role of xSox6, we analyzed neural crest markers in xSox6-depleted embryos. Whole-mount in situ hybridization demonstrated that the expression patterns of *xFoxD3* (Fig. 5A) and *xTwist* (Fig. 5B) were not substantially affected by xSox6 knockdown. These results indicate that xSox6 is dispensable for the induction and migration of neural crest cells. We then analyzed chondrocyte markers. qRT-PCR analysis showed that the strong induction of *xMatn1* and *xAgc1* during chondrogenesis was inhibited in xSox6-depleted embryos (Fig. 5C). Whole-mount in situ hybridization also showed that these two chondrocyte markers were drastically downregulated in xSox6-depleted embryos (Fig. 5D). Thus, xSox6 is essential for chondrocyte differentiation but not for neural crest formation and migration. This phenotype of

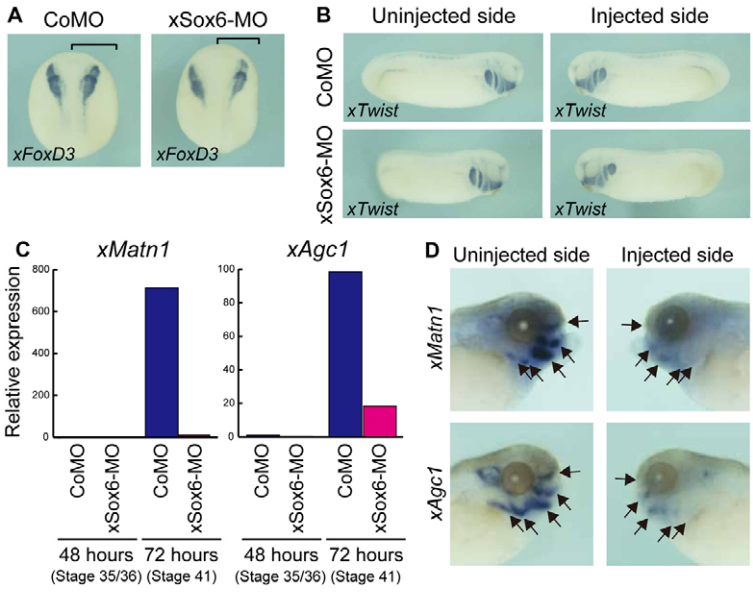

Fig. 5. xSox6 is required for chondrocyte differentiation but not for neural crest development. (**A**,**B**) xSox6-MO or CoMO was injected unilaterally into the animal pole of two blastomeres (10 ng/cell) at the four-cell stage, and the embryos were fixed at stages 17 (A) and 25 (B). Whole-mount in situ hybridization was performed with xFoxD3 (A) and xTwist (B) probes. Brackets indicate the injected side. Frequency of specimen with the indicated phenotype (nearly equal expression) was CoMO in A, 5/5; xSox6-MO in A, 18/21; CoMO in B, 5/5; xSox6-MO in B, 11/11. (**C**) xSox6-MO or CoMO was injected into the animal pole of all blastomeres (10 ng/cell) at the four-cell stage. Embryo heads were harvested 48 and 72 hours after fertilization (stages 35/36 and 41, respectively). The expression levels of chondrocyte markers xMatn1 and xAgc1 were analyzed by qRT-PCR. Representative results from two independent experiments are shown. (**D**) xSox6-MO was injected unilaterally into the animal pole of two blastomeres (10 ng/cell) at the four-cell stage, and the embryos were fixed at stage 41. Whole-mount in situ hybridization was performed with xMatn1 and xAgc1 probes. Arrows indicate presumptive cartilaginous elements. Frequency of specimen with the indicated phenotype (markedly reduced expression) was Matn1, 11/12; Agc1, 10/10.

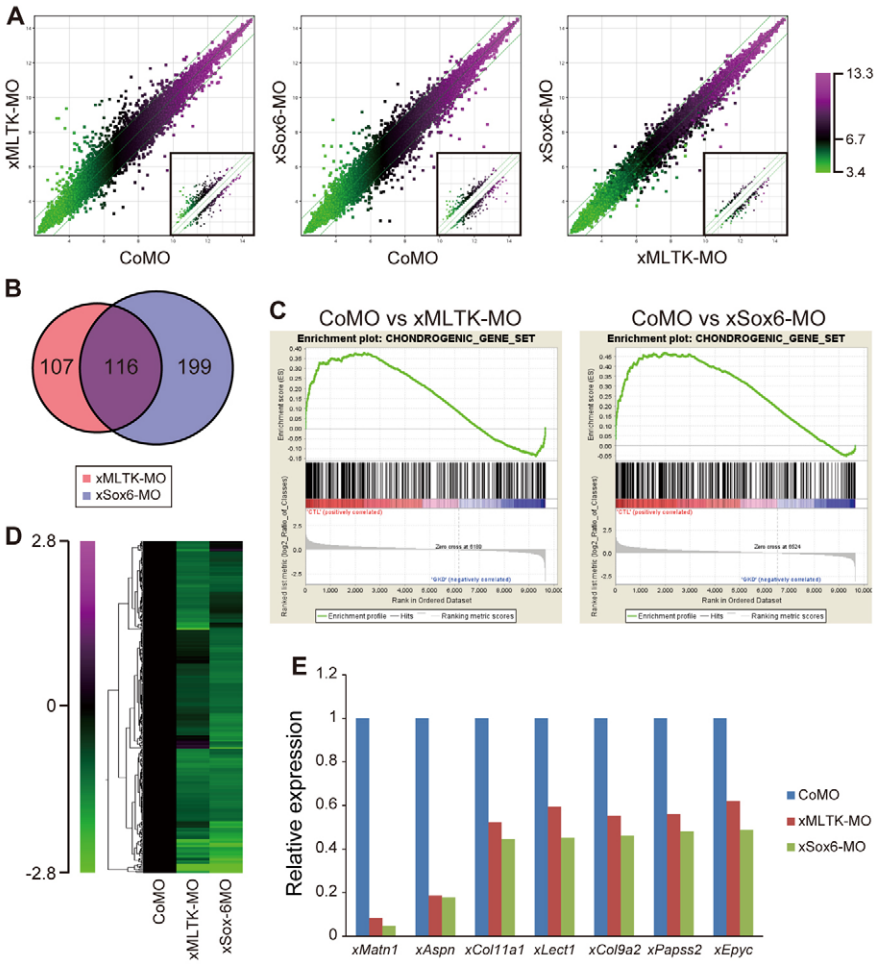

Fig. 6. Genome-wide gene expression analysis of xMLTK- and xSox6-depleted embryos. CoMO, xMLTK-MO, or xSox6-MO was injected into the animal pole of all blastomeres (10 ng/cell) at the four-cell stage. The heads of embryos were cut out and harvested at 72 hours after fertilization (corresponding to stage 41). (**A**) Scatter plots showing signal intensity of all probe sets, which is represented by color according to the log scale on the right. Inset scatter plots show only the dots representing probe sets whose signal intensity changed more than twofold. (**B**) Venn diagram of the number of genes whose expression levels were more than halved in xMLTK-MO- or xSox6-MO-injected embryos. (**C**) Gene set enrichment analysis was performed to assess overrepresentation of chondrogenic gene set. The bottom region of the plot shows the log ratio of signal intensity of each gene in CoMO-injected embryos to that in xMLTK-MO- or xSox6-MO-injected embryos. Genes were ranked from left to right according to the ratio. The middle region shows where the genes in the chondrogenic gene set appear in the ranked list. The top region shows the running enrichment score (ES) for the chondrogenic gene set, calculated by walking down the ranked list of genes from left to right, increasing a running-sum statistic when a gene is in the gene set and decreasing it when it is not. The score at the peak is the ES. The normalized ES and *P*-value in CoMO versus xMLTK-MO are 1.4 and less than 0.001, respectively, and those in CoMO versus xSox6-MO are 1.7 and less than 0.001, respectively. (**D**) Expression profiles of genes whose expression levels were more than halved in xMLTK-MO- or xSox6-MO-injected embryos. The ratio of signal intensity in xMLTK or xSox6 morphants relative to that in control morphants is represented by color according to the scale on the left. Genes were rearranged by clustering analysis. (**E**) Signal intensity of cartilage-expressed genes in xMLTK-MO- and xSox6-MO-injected embryos relative to that in CoMO-injected embryos.

xSox6-depleted embryos is essentially the same as that of xMLTK-depleted embryos. Therefore, these results together suggest that xMLTK regulates chondrogenesis through induction of *xSox6*.

xSox6-depleted embryos closely resemble xMLTK-depleted embryos in the gene expression profile

To further characterize the phenotypes of xMLTK-depleted and xSox6-depleted embryos, we performed genome-wide gene expression analysis. The heads of embryos injected with CoMO, xMLTK-MO or xSox6-MO were collected at stage 41 and used for microarray analysis. Scatter plot analysis showed a close similarity between xMLTK-MO and xSox6-MO-injected embryos in the gene expression profile (Fig. 6A). A Venn diagram demonstrated a remarkable overlap between xMLTK-dependent and xSox6-dependent genes (Fig. 6B). Gene set enrichment analysis (Subramanian et al., 2005) showed that genes whose mouse orthologs were induced during chondrogenesis in vivo (Cameron et al., 2009) were highly enriched in both the subsets of xMLTK-dependent and xSox6-dependent genes (Fig. 6C). Clustering analysis also revealed that the subsets of xSox6-dependent genes closely resemble those of xMLTK-dependent genes (Fig. 6D). Moreover, there was a remarkably high correlation between xMLTK-MO- and xSox6-MO-injected embryos in the expression levels of cartilage-expressed genes, such as *Matn1*, *Col11a1* (Li et al., 1995), *Lect1* (Shukunami et al., 1999), *Col9a2* (Muragaki et al., 1996; Annunen et al., 1999), *Papss2* (Stelzer et al., 2007), *Epyc*

(Johnson et al., 1999) and *Aspn* (Henry et al., 2001) (Fig. 6E). These observations strongly suggest that xMLTK and xSox6 regulate the same subsets of genes involved in chondrogenesis.

xMLTK regulates chondrogenesis through p38 and JNK pathways

Previous reports showed that MLTK activates both the p38 MAPK and JNK pathways (Gotoh et al., 2001; Gross et al., 2002). Therefore, we performed rescue experiments with constitutively active forms of *xMKK6* (a direct activator of p38) and *xMKK7* (a direct activator of JNK) (CA-x*MKK6* and CA-x*MKK7*) in order to investigate whether p38 and JNK pathways are involved in chondrogenesis as downstream signaling effectors of xMLTK. Co-injection of HA-CA-*xMKK6* or HA-CA-*xMKK7* plasmid with xMLTK-MO significantly restored the size of cartilage when compared with siblings that received injection of xMLTK-MO alone (Fig. 7A,B). These results suggest that xMLTK chondrogenic activity is dependent upon p38 and JNK signaling pathways.

DISCUSSION

Cartilages are formed as the first skeleton of the embryo before endochondral bone formation, and also function in joints, airways and ears of adults as a supporting organ that has the flexibility. Therefore, abnormalities in chondrogenesis cause congenital disorders in human, such as campomelic dysplasia and dwarfism. In this study, we show that MLTK plays an essential role in chondrocyte differentiation during embryonic development through inducing Sox6, which is shown to be an essential transcription factor for chondrogenesis in *Xenopus*. Thus, xMLTK depletion resulted in complete loss of Meckel's cartilage, which is derived from only neural crest cells (Sadaghiani and Thiébaud, 1987), and drastic reduction of ceratohyal and ceratobranchial cartilages, which are derived from neural crest and mesodermal cells. Importantly, the formation, migration and maintenance of neural crest cells were normal in xMLTK-depleted embryos, indicating that xMLTK is specifically required for a differentiation process of neural crest cells into chondrocytes. Although the mechanism of neural crest formation and migration has been studied extensively, how neural crest cells differentiate into chondrocytes remains poorly understood in organisms. Our findings introduce xMLTK as a key signaling factor in the differentiation of neural crest cells into chondrocytes.

Sox5, Sox6 and Sox9 play a central role in chondrocyte differentiation in mice (Lefebvre and Smits, 2005). Although Sox9 is required for both mesenchymal condensations and subsequent chondrocyte differentiation, Sox5 and Sox6 are specifically required for chondrocyte differentiation in mouse embryonic development (Smits et al., 2001; Akiyama et al., 2002). Interestingly, xMLTK depletion resulted in marked suppression of *xSox6* expression at stage 41, but it did not affect the expression of *xSox5* and *xSox9*. However, xSox6 function was unknown in *Xenopus*. Our analysis then shows that *xSox6* expression markedly increases in the prospective cartilage at around stage 39, when pre-cartilaginous condensations are occurring (Kerney et al., 2007; Lee and Saint-Jeannet, 2011), and that chondrocyte differentiation is severely inhibited in xSox6-depleted embryos, whereas prior neural crest development is normal. These results indicate that xSox6 is specifically required for chondrocyte differentiation, very similar to xMLTK. Collectively, our results show that xMLTK is required for *xSox6* expression, which is essential for chondrocyte differentiation.

In mice, although Sox9 is required for *Sox5* and *Sox6* expression in chondrogenesis (Akiyama et al., 2002; Ikeda et al., 2004), the mechanism by which Sox9 induces *Sox5* and *Sox6* expression remains unknown. We have found that ectopic expression of *xMLTK* can induce *xSox6* expression in a *xSox9*-dependent manner. Moreover, using the in vitro model system of cartilage formation, we showed that *xSox6* induction by xMLTK requires xSox9. Based on these findings, we propose a hypothetical model in which xMLTK activates xSox9, thereby inducing *xSox6* expression and promoting chondrocyte differentiation. It has been reported that p38 signaling can increase the transcriptional activity of Sox9, and transgenic mice in which p38 signaling is constitutively activated in chondrocytes, show phenotypes similar to those of mice that overexpress *Sox9* in chondrocytes (Zhang et al., 2006). In addition, many reports have suggested that the p38 pathway is a positive regulator of the differentiation of mesenchymal cells into chondrocytes (Bobick and Kulyk, 2008). Our analysis suggests that p38 and JNK MAPK pathways play an important role as downstream signaling components of xMLTK during chondrogenesis. It would be intriguing to examine upstream modulators of xMLTK activity. It has been reported that EGF treatment of cultured cells promotes nuclear accumulation of MLTKα and phosphorylation of MAPK-targeted transcription factors (Cho et al., 2004). However, what ligand activates xMLTK during chondrogenesis remains unclear. Thus, the mechanism by which xMLTK is activated should await further investigation.

This study examines the expression patterns of chondrocyte markers, *xMatn1*, *xAgc1* and *xCrt1*, which are established markers in mice (Lefebvre and Smits, 2005). To our knowledge,

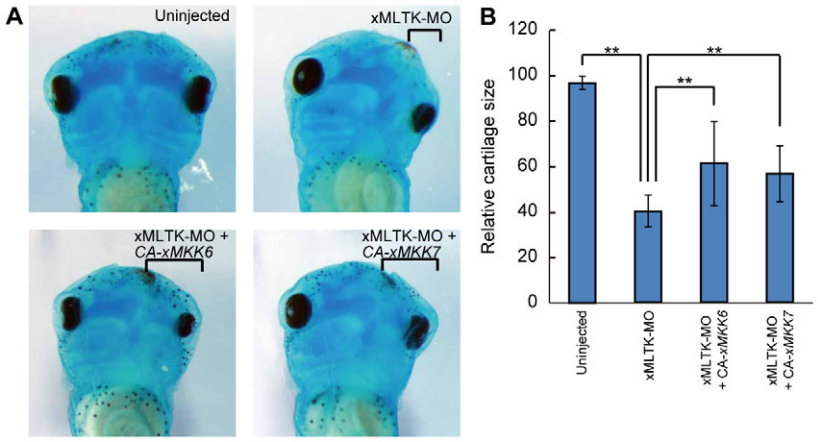

Fig. 7. p38 and JNK pathways function downstream of xMLTK during chondrogenesis. (**A**) xMLTK-MO (*n*=33), xMLTK-MO plus HA-CA-xMKK6 plasmid (n=29) or xMLTK-MO plus HA-CA-xMKK7 plasmid (*n*=33) was injected unilaterally into the animal pole of two blastomeres (xMLTK-MO, 10 ng/cell; plasmid, 50 pg /cell) at the four-cell stage. Uninjected embryos (n=38) and injected embryos were fixed at stage 45, and cartilages were stained with Alcian Blue. Brackets indicate the injected side. (**B**) The relative cartilage size (the rate of the length of the right side to that of the left side of ceratohyal cartilages) was quantified. Values are means±s.d. ***P*<0.01.

this is the first to describe the expression patterns of chondrocyte markers in *Xenopus laevis*. Our analysis revealed that the expression of chondrocyte markers is first detected in the prospective craniofacial cartilage at stage 39, when pre-cartilaginous condensations are occurring (Kerney et al., 2007; Lee and Saint-Jeannet, 2011). *xSox6* expression begins to increase at around stage 35/36 and then markedly increases at stage 39 in the prospective cartilage, while *xSox5* and *xSox9* are continuously expressed in the neural crest from the neurula stage to the late tailbud stage. Thus, studies examining spatiotemporal expression patterns of chondrocyte markers and key transcription factors complement functional analysis of the factors involved in chondrogenesis, suggesting that *Xenopus laevis* is a useful model organism to study the mechanism of the differentiation of neural crest cells into chondrocytes.

In conclusion, this study identifies a novel player, xMLTK, in chondrogenesis, and reveals that xMLTK functions to trigger the induction of *xSox6* by xSox9 in chondrogenesis during embryonic development.

Acknowledgements
We thank S. Nishimoto, T. Endo, T. Araki, K. Miyatake and members of the Nishida laboratory for technical advice and helpful discussion.

Funding
This work was supported by grants from the Ministry of Education, Culture, Sports, Science and Technology of Japan and Core Research for Evolutional Science and Technology (CREST), Japan Science and Technology (to E.N.). T.S. is a Research Fellow of the Japan Society for the Promotion of Science.

Competing interests statement
The authors declare no competing financial interests.

Supplementary material
Supplementary material available online at
http://dev.biologists.org/lookup/suppl/doi:10.1242/dev.078675/-/DC1

References

Akiyama, H., Chaboissier, M. C., Martin, J. F., Schedl, A. and de Crombrugghe, B. (2002). The transcription factor Sox9 has essential roles in successive steps of the chondrocyte differentiation pathway and is required for expression of Sox5 and Sox6. *Genes Dev.* **16**, 2813-2828.

Annunen, S., Paassilta, P., Lohiniva, J., Perälä, M., Pihlajamaa, T., Karppinen, J., Tervonen, O., Kröger, H., Lähde, S., Vanharanta, H. et al. (1999). An allele of COL9A2 associated with intervertebral disc disease. *Science* **285**, 409-412.

Bi, W., Deng, J. M., Zhang, Z., Behringer, R. R. and de Crombrugghe, B. (1999). Sox9 is required for cartilage formation. *Nat. Genet.* **22**, 85-89.

Bloem, L. J., Pickard, T. R., Acton, S., Donoghue, M., Beavis, R. C., Knierman, M. D. and Wang, X. (2001). Tissue distribution and functional expression of a cDNA encoding a novel mixed lineage kinase. *J. Mol. Cell. Cardiol.* **33**, 1739-1750.

Bobick, B. E. and Kulyk, W. M. (2008). Regulation of cartilage formation and maturation by mitogen-activated protein kinase signaling. *Birth Defects Res. C Embryo Today* **84**, 131-154.

Cameron, T. L., Belluoccio, D., Farlie, P. G., Brachvogel, B. and Bateman, J. F. (2009). Global comparative transcriptome analysis of cartilage formation in vivo. *BMC Dev. Biol.* **9**, 20.

Chang, L. and Karin, M. (2001). Mammalian MAP kinase signalling cascades. *Nature* **410**, 37-40.

Cho, Y. Y., Bode, A. M., Mizuno, H., Choi, B. Y., Choi, H. S. and Dong, Z. (2004). A novel role for mixed-lineage kinase-like mitogen-activated protein triple kinase alpha in neoplastic cell transformation and tumor development. *Cancer Res.* **64**, 3855-3864.

Christe, M., Jin, N., Wang, X., Gould, K. E., Iversen, P. W., Yu, X., Lorenz, J. N., Kadambi, V., Zuckerman, S. H. and Bloem, L. J. (2004). Transgenic mice with cardiac-specific over-expression of MLK7 have increased mortality when exposed to chronic beta-adrenergic stimulation. *J. Mol. Cell. Cardiol.* **37**, 705-715.

Furue, M., Myoishi, Y., Fukui, Y., Ariizumi, T., Okamoto, T. and Asashima, M. (2002). Activin A induces craniofacial cartilage from undifferentiated Xenopus ectoderm in vitro. *Proc. Natl. Acad. Sci. USA* **99**, 15474-15479.

Gallo, K. A. and Johnson, G. L. (2002). Mixed-lineage kinase control of JNK and p38 MAPK pathways. *Nat. Rev. Mol. Cell Biol.* **3**, 663-672.

Gotoh, I., Adachi, M. and Nishida, E. (2001). Identification and characterization of a novel MAP kinase kinase kinase, MLTK. *J. Biol. Chem.* **276**, 4276-4286.

Gross, E. A., Callow, M. G., Waldbaum, L., Thomas, S. and Ruggieri, R. (2002). MRK, a mixed lineage kinase-related molecule that plays a role in gamma-radiation-induced cell cycle arrest. *J. Biol. Chem.* **277**, 13873-13882.

Han, Y. and Lefebvre, V. (2008). L-Sox5 and Sox6 drive expression of the aggrecan gene in cartilage by securing binding of Sox9 to a far-upstream enhancer. *Mol. Cell. Biol.* **28**, 4999-5013.

Henry, S. P., Takanosu, M., Boyd, T. C., Mayne, P. M., Eberspaecher, H., Zhou, W., de Crombrugghe, B., Hook, M. and Mayne, R. (2001). Expression pattern and gene characterization of asporin. a newly discovered member of the leucine-rich repeat protein family. *J. Biol. Chem.* **276**, 12212-12221.

Hopwood, N. D., Pluck, A. and Gurdon, J. B. (1989). A Xenopus mRNA related to Drosophila twist is expressed in response to induction in the mesoderm and the neural crest. *Cell* **59**, 893-903.

Ikeda, T., Kamekura, S., Mabuchi, A., Kou, I., Seki, S., Takato, T., Nakamura, K., Kawaguchi, H., Ikegawa, S. and Chung, U. I. (2004). The combination of SOX5, SOX6, and SOX9 (the SOX trio) provides signals sufficient for induction of permanent cartilage. *Arthritis Rheum.* **50**, 3561-3573.

Johnson, J., Shinomura, T., Eberspaecher, H., Pinero, G., Decrombrugghe, B. and Höök, M. (1999). Expression and localization of PG-Lb/epiphycan during mouse development. *Dev. Dyn.* **216**, 499-510.

Kerney, R., Gross, J. B. and Hanken, J. (2007). Runx2 is essential for larval hyobranchial cartilage formation in Xenopus laevis. *Dev. Dyn.* **236**, 1650-1662.

Le Douarin, N. M., Creuzet, S., Couly, G. and Dupin, E. (2004). Neural crest cell plasticity and its limits. *Development* **131**, 4637-4650.

Lee, Y. H. and Saint-Jeannet, J. P. (2011). Sox9 function in craniofacial development and disease. *Genesis* **49**, 200-208.

Lefebvre, V. and Smits, P. (2005). Transcriptional control of chondrocyte fate and differentiation. *Birth Defects Res. C Embryo Today* **75**, 200-212.

Lefebvre, V., Li, P. and de Crombrugghe, B. (1998). A new long form of Sox5 (L-Sox5), Sox6 and Sox9 are coexpressed in chondrogenesis and cooperatively activate the type II collagen gene. *EMBO J.* **17**, 5718-5733.

Li, Y., Lacerda, D. A., Warman, M. L., Beier, D. R., Yoshioka, H., Ninomiya, Y., Oxford, J. T., Morris, N. P., Andrikopoulos, K. and Ramirez, F. (1995). A fibrillar collagen gene, Col11a1, is essential for skeletal morphogenesis. *Cell* **80**, 423-430.

Liu, T. C., Huang, C. J., Chu, Y. C., Wei, C. C., Chou, C. C., Chou, M. Y., Chou, C. K. and Yang, J. J. (2000). Cloning and expression of ZAK, a mixed lineage kinase-like protein containing a leucine-zipper and a sterile-alpha motif. *Biochem. Biophys. Res. Commun.* **274**, 811-816.

Martin, B. L. and Harland, R. M. (2001). Hypaxial muscle migration during primary myogenesis in Xenopus laevis. *Dev. Biol.* **239**, 270-280.

Muragaki, Y., Mariman, E. C., van Beersum, S. E., Perälä, M., van Mourik, J. B., Warman, M. L., Olsen, B. R. and Hamel, B. C. (1996). A mutation in the gene encoding the alpha 2 chain of the fibril-associated collagen IX, COL9A2, causes multiple epiphyseal dysplasia (EDM2). *Nat. Genet.* **12**, 103-105.

Nagy, A., Kénesi, E., Rentsendorj, O., Molnár, A., Szénási, T., Sinkó, I., Zvara, A., Oommen, S. T., Barta, E., Puskás, L. G. et al. (2011). Evolutionarily conserved, growth plate zone-specific regulation of the matrilin-1 promoter: L-Sox5/Sox6 and Nfi factors bound near TATA finely tune activation by Sox9. *Mol. Cell. Biol.* **31**, 686-699.

Ng, L. J., Wheatley, S., Muscat, G. E., Conway-Campbell, J., Bowles, J., Wright, E., Bell, D. M., Tam, P. P., Cheah, K. S. and Koopman, P. (1997). SOX9 binds DNA, activates transcription, and coexpresses with type II collagen during chondrogenesis in the mouse. *Dev. Biol.* **183**, 108-121.

Nieuwkoop, P. D. and Faber, J. (1967). *Normal Table of Xenopus laevis (Daudin)*. Amsterdam: North Holland.

Nishida, E. and Gotoh, Y. (1993). The MAP kinase cascade is essential for diverse signal transduction pathways. *Trends Biochem. Sci.* **18**, 128-131.

Pohl, B. S. and Knöchel, W. (2001). Overexpression of the transcriptional repressor FoxD3 prevents neural crest formation in Xenopus embryos. *Mech. Dev.* **103**, 93-106.

Robinson, M. J. and Cobb, M. H. (1997). Mitogen-activated protein kinase pathways. *Curr. Opin. Cell Biol.* **9**, 180-186.

Sadaghiani, B. and Thiébaud, C. H. (1987). Neural crest development in the Xenopus laevis embryo, studied by interspecific transplantation and scanning electron microscopy. *Dev. Biol.* **124**, 91-110.

Sasai, N., Mizuseki, K. and Sasai, Y. (2001). Requirement of FoxD3-class signaling for neural crest determination in Xenopus. *Development* **128**, 2525-2536.

Sauka-Spengler, T. and Bronner-Fraser, M. (2008). A gene regulatory network orchestrates neural crest formation. *Nat. Rev. Mol. Cell Biol.* **9**, 557-568.

Shukunami, C., Iyama, K., Inoue, H. and Hiraki, Y. (1999). Spatiotemporal pattern of the mouse chondromodulin-I gene expression and its regulatory role in vascular invasion into cartilage during endochondral bone formation. *Int. J. Dev. Biol.* **43**, 39-49.

Sive, H. L., Grainger, R. M. and Harland, R. M. (2000). *Early Development of Xenopus laevis: A Laboratory Manual*. New York: Cold Spring Harbor Laboratory Press.

Smits, P., Li, P., Mandel, J., Zhang, Z., Deng, J. M., Behringer, R. R., de Crombrugghe, B. and Lefebvre, V. (2001). The transcription factors L-Sox5 and Sox6 are essential for cartilage formation. *Dev. Cell* **1**, 277-290.

Spokony, R. F., Aoki, Y., Saint-Germain, N., Magner-Fink, E. and Saint-Jeannet, J. P. (2002). The transcription factor Sox9 is required for cranial neural crest development in Xenopus. *Development* **129**, 421-432.

Stelzer, C., Brimmer, A., Hermanns, P., Zabel, B. and Dietz, U. H. (2007). Expression profile of Papss2 (3′-phosphoadenosine 5′-phosphosulfate synthase 2) during cartilage formation and skeletal development in the mouse embryo. *Dev. Dyn.* **236**, 1313-1318.

Subramanian, A., Tamayo, P., Mootha, V. K., Mukherjee, S., Ebert, B. L., Gillette, M. A., Paulovich, A., Pomeroy, S. L., Golub, T. R., Lander, E. S. et al. (2005). Gene set enrichment analysis: a knowledge-based approach for interpreting genome-wide expression profiles. *Proc. Natl. Acad. Sci. USA* **102**, 15545-15550.

Wang, X., Mader, M. M., Toth, J. E., Yu, X., Jin, N., Campbell, R. M., Smallwood, J. K., Christe, M. E., Chatterjee, A., Goodson, T. et al. (2005). Complete inhibition of anisomycin and UV radiation but not cytokine induced JNK and p38 activation by an aryl-substituted dihydropyrrolopyrazole quinoline and mixed lineage kinase 7 small interfering RNA. *J. Biol. Chem.* **280**, 19298-19305.

Yamanaka, H., Moriguchi, T., Masuyama, N., Kusakabe, M., Hanafusa, H., Takada, R., Takada, S. and Nishida, E. (2002). JNK functions in the non-canonical Wnt pathway to regulate convergent extension movements in vertebrates. *EMBO Rep.* **3**, 69-75.

Zhang, R., Murakami, S., Coustry, F., Wang, Y. and de Crombrugghe, B. (2006). Constitutive activation of MKK6 in chondrocytes of transgenic mice inhibits proliferation and delays endochondral bone formation. *Proc. Natl. Acad. Sci. USA* **103**, 365-370.

Zhao, Q., Eberspaecher, H., Lefebvre, V. and De Crombrugghe, B. (1997). Parallel expression of Sox9 and Col2a1 in cells undergoing chondrogenesis. *Dev. Dyn.* **209**, 377-386.

A

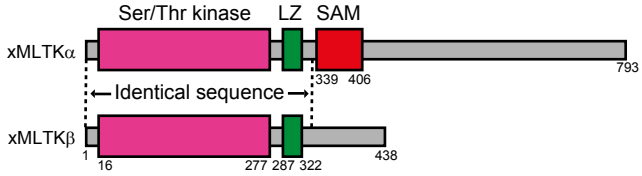

B

xMLTKα

```
Homo sapiens      1 MGSLGASFVQIKFDDLQFENCGGGSFGSVYRAKWISQDEVAVKKLLKIEKEAEILSVL 60
Mus musculus      1 MGSLGASFVQIKFDDLQFENCGGGSFGSVYRAKWISQDEVAVKKLLKIEKEAEILSVL 60
Gallus gallus     1 MGSTSASFVQIRFDDLQFENCGGGSFGSVYRAKWISQDEVAVKKLLKIEKEAEILSVL 60
Xenopus laevis    1 MGSHTASFVQIKFDDLQFENCGGGSFGSVYRAKWISQDEVAVKKLLKIEKEAEILSVL 60
Danio rerio       1 MASLGSSFVQIKFDDLQFENCGGGSFGSVYRAKWISQDEVAVKKLLKIEKEAEILSVL 60

Homo sapiens     61 SHRNIIQFYGVILEPNYGIVTEYASLGSLVDYINSNRSEEMDMDHIMKWATDVAKGMHY 120
Mus musculus     61 SHRNIIQFYGVILEPNYGIVTEYASLGSLVDYINSNRSEEMDMDHIMKWATDVAKGMHY 120
Gallus gallus    61 SHRNIIQFYGAVLEPNYGIVTEYASLGSLVDYINSNKSEEMDMDHIMKWATDIAKGMHY 120
Xenopus laevis   61 SHRNIIQFYGAVLEPNYGIVTEYASLGSLVDYINSARSEEMDMDHIMKWATDIAKGMHY 120
Danio rerio      61 SHRNIIKFYGAILEPNYGIVTEYASGSLFDMLSDDSDDISMSQQIMKWATDIAKGMHY 120

Homo sapiens    121 LHMEAPVKVIHRDLKSRNVVIADDGVLKICDFGASRFHNHTTHMSLVGTFPWMAPEVIQS 180
Mus musculus    121 LHMEAPVKVIHRDLKSRNVVIADDGVLKICDFGASRFHNHTTHMSLVGTFPWMAPEVIQS 180
Gallus gallus   121 LHMEAPVKVIHRDLKSRNVVIADDGVLKICDFGASRFHNHTTHMSLVGTFPWMAPEVIQS 180
Xenopus laevis  121 LHMEAPIKVIHRDLKSRNVVITVDGVLKICDFGASRFHNHTTHMSLVGTFPWMAPEVIQS 180
Danio rerio     121 LHSEAPVKVIHRDLKSRNVVLSSDSVLKICDFGASKFHNHTTHMSLVGTFPWMAPEVIQS 180

Homo sapiens    181 LPVSETCDTYSYGVVLWEMLTREVPFKGLEGLQVAWLVVEKNERLTIPSSCPRSFAELLH 240
Mus musculus    181 LPVSETCDTYSYGVVLWEMLTREVPFKGLEGLQVAWLVVEKNERLTIPSSCPRSFAELLH 240
Gallus gallus   181 LPVSETCDTYSYGVVLWEMLTREVPFKGLEGLQVAWLVVEKNERLTIPSSCPRSFAELMH 240
Xenopus laevis  181 LPVSETCDTYSYGVVLWEMLTREVPFKGLEGLQVAWLVVEKNERLTIPSSCPRSFAELMH 240
Danio rerio     181 LPVSETCDTYSYGVVLWEMLTQEIPFKGLEGLQVAWLVVEKNERLTIPSSCPASFAQLMR 240

Homo sapiens    241 QCWEADARKRPSFKQIISFLESMSNDTSLPDKCNSFLHNKAEWRCEIEATLERLKRLERD 300
Mus musculus    241 QCWEADARKRPSFKQIISFLESMSNDTNLPDKCNSFLHNKAEWRCEIEATLERLKRLERD 300
Gallus gallus   241 QCWEADSKRPSFKQIISFLESMSNDSKLPDKCNSFLHNKAEWRCEIEPTLERLKRLERD 300
Xenopus laevis  241 QCWEADSKRPSFKQILSFLESMSNDSKLPDKCNSFLHNKAEWRCEIEPTLERLKRLERD 300
Danio rerio     241 SCWATEPQRPSFKHILSTLESMSNSTQLPDKCNTFLQNKAEWRCEIEATLERLKRLERD 300

Homo sapiens    301 LSPKEQEIKERERRLKQWEKKLTEQSNTPLLPSFPEGAVTDDEVKCVVQCLVRKGDSSAE 360
Mus musculus    301 LSPKEQEIKERERRLKQWEKKLTEQSNTPLLPSFPEGAVTDDEVKFVVQCLVRKGESSVE 360
Gallus gallus   301 LSPKEQELKERERRLKQWEKKLTEQSNTPLLPSFDECAVTDEIVFEVMQCLTRKGDASGE 360
Xenopus laevis  301 LSYKEQELKERERRLKLWEKKLTEQSNTPLLPSFDECSVTDEIVFVVMQCLVKSDDENI- 359
Danio rerio     301 LSTSEQALKERERRLKQWERKLIEQSNTPLLPNLAEHSVTDEHQHEIMQFIF---EGDGE 357

Homo sapiens    361 MSVVASLSKENNITGKRLLLLDEDLKDVGIVSKGHIIEFKSHIEKLTHDYINLFHFPPL 420
Mus musculus    361 MSGVASLSKENNITGKRLLLLDEDLKDVGIVSKGHIIEFKSHIEKLTHDYINLFHFPPL 420
Gallus gallus   361 MSAVASLSKEHHITGKRLLLLDEDLKDVGIISKGHIIEFKTAIEKLTHDYINLFHFPPL 420
Xenopus laevis  360 ----VASLSRQHHITGKRLLLLDRDLKDVGIVSKGHIIEFKTAIEKLTHDYINLFHFPPL 416
Danio rerio     358 LQQVTNVSRQNHITGQRLLLLDSDMRDLGVISKGHIIELKTPIEKLTHDYINLFHFPPL 417

Homo sapiens    421 IKDSGGEPEENEE--KVVNLELVFGPHPKPGPGQDCKWKMYMEDDGDEVAIPVIKDVTF 478
Mus musculus    421 IKDSGGEPEENEE--KVVNLELVFGPHPKPGPGQDCKWKMYMEDDGDEVAIPVIKDVTF 478
Gallus gallus   421 IKDSAGEAEENIE--KVVNLELVFGPHPKLGWGPKDCKWKMYMEDDGDEIAIPVIKDVTF 478
Xenopus laevis  417 IKDLESE-NDDEE--KVVNLELVFGPHPKPGCSCPEDCKWKMYMEDDGDEIAIPVIKDVTF 473
Danio rerio     418 IKDGSASEEADEDWSKVVNLELVFGPHPKAGTGQKDCKWKMYMEDDGDEVAIPVIKDVTF 477

Homo sapiens    479 NTNLPDAEILKMTKPPFVMDKWIVGIAKSQTVECTVTYESDVRTPRSFRPVHSIQMSRTK 538
Mus musculus    479 NTSLPDAEILKMTKPPFVMDKWIVGIAEDQTVECTVTYENDVRTPRLFRPVHSIQMDRTK 538
Gallus gallus   479 NTNLPDVELLKMTKPPFVMDKWIVGIEEHQSVECTVTYESDVRAPKSFRPVQAIQMSKVK 538
Xenopus laevis  474 NRNQPDVELLRMTKPPFVMDKWIVGIRENETVECTVTYENDVRTPRIFRPIHKIHQDRMK 533
Danio rerio     478 NANRPDVDVLRMTKPPFVMDKWIVGISGTHTVDYEMHTEGWMKSPKCPRPVHTVQMSADS 537

Homo sapiens    539 PQDEVSAVQMAHQTLFTNSDGNPGSRSDSSADCQNLDTLRMPCIASNTS-------LQRSQ 592
Mus musculus    539 PQDEVSAVQMAHQTLFSSSEGNPGSRSDSSADCQNLDTLRMPCIASHTS-------LQRSQ 592
Gallus gallus   539 AQDEVSAVQMAHQTSLPNSEGHSRSRVSSICSQNMQTLRMHCIAKAIS-------LQHGD 592
Xenopus laevis  534 MQDAESPVQMAHMSPLLTSES-KQSNYESSPCCQNIYTLRMPCMANPTSPQHAAGLPRSQ 592
Danio rerio     538 GRDVISPVQLFVDKTAPGIREAHNRSRSNSGVLPKNIYSLRMKCMKEQAA-------QESP 590

Homo sapiens    593 SN-PILGSPFFSHFDGQDSYAAAVRRPQVPIKYQQITP-VNQSRSSSPTQYGPTKNFSSL 650
Mus musculus    593 SN-PILGSPFFYFANDQDSYAAAVRRTQIFVKYQQITPSINPSRSSSPTQYGPSRNFSSL 651
Gallus gallus   593 PHSETTVSHYLPYLQSQDSYAAAVRRTRGFVNY-HYTS-ISHGRSSSPLSHSPVRNLSSL 650
Xenopus laevis  593 SSSLSNLSQILPYLQSQESYAAAVRRIRASPTL-QVTS-INYSRSSSPTQFGPAKNLSSL 650
Danio rerio     591 SK--MSLPQFLSVISNQESYAAAVRRSPNRSP----LSP-WTDSRSSSPF---PSVKLSNM 641

Homo sapiens    651 HL-NSRDSGFSSGNTDTSSERGYSDRSRNKYGRGSISLNSSPRGRYSGKSQHSTPSRGR 709
Mus musculus    652 NL-SSRDSGFSSLN-DSSERGYSDRSRNKYYRGSVSLNSSPKGRYGGKSQHSTPSRKR 709
Gallus gallus   651 HI-NSRGSSTSSTASDTASERDPSTGKARNASHSGNSR---SSSDGR----RSGTSSGVPPR 704
Xenopus laevis  651 SIQSSRGSSASSTASDPSERDPAHRTSNNSYYK---HNRYSTPVHR----RSGGKSG---QM 703
Danio rerio     642 HL-GSRGSPSSITSESASERDPPSAGAKHNYN-KKPYYDHHTLK-MSSRGDGEP-RRF 697

Homo sapiens    710 YPGKFYDVSQSALNPHQSPDFKRSP---RDLHQFNTPGVPLHPTDSRASEKDSKVSEG 767
Mus musculus    710 YSGKFYDVLPQSALNTHQSPDFKRSPNDHDRRVPTIPGVPLHPTASKAGEKESRVSEG 769
Gallus gallus   705 SSGRAGR-TASMPAHEQRRYERNS-----PQKHLPGVPLQPSEPRRSEGGRASESG 758
Xenopus laevis  704 NSGRWYK-SYTTTYNESRPNEQRPQ---KTMQNRHLPGVPLKPSDTDVNGGEKNTNEG 758
Danio rerio     698 LPQRGSRGYQHAGRPRNAHSYATPE-----HYQRDLPGVSMAAE-GPKQKVASEEPGLGD 751

Homo sapiens    768 QTKVEYRKKPHRP-SPAKTNKERARGDRGRGNF------ 800
Mus musculus    770 QTKVEYRKKPHRQ-LSAKTSKERTRGMYRGRGNF------ 802
Gallus gallus   759 QTKVQHVKKPHRQ-STGKQGKERPKGSWRGRGAF------ 791
Xenopus laevis  759 QTKVDYSKKPHKQTTTSKSHKDRSKSFGRGRGSWL---- 793
Danio rerio     752 QTKVE-RKKPHKQECKYQEVRPVRGRSRGCRGGGRGRN 789
```

xMLTKβ

```
Homo sapiens      1 MGSLGASFVQIKFDDLQFFENCGGGSFGSVYRAKWISQDEVAVKKLLKIEKEAEILSVL 60
Mus musculus      1 MGSLGASFVQIKFDDLQFFENCGGGSFGSVYRAKWISQDEVAVKKLLKIEKEAEILSVL 60
Xenopus laevis    1 MGSLTASFVQIKFDDLQFFENCGGGSFGSVYRAKWISQDKEVAVKKLLKIEKEAEILSVL 60

Homo sapiens     61 SHRNIIQFYGVILEPNYGIVTEYASLGSLYDYINSNRSEPMDMQHIMKWATDVAKGMHY 120
Mus musculus     61 SHRNIIQFYGVILEPNYGIVTEYASLGSLYDYINSNRSEPMDMQHIMKWATDVAKGMHY 120
Xenopus laevis   61 SHRNIIQFYGAVLEPNYGIVTEYACGSLYDYINSARSEPMDMQHIMKWATDVAKGMHY 120

Homo sapiens    121 LHMEAPVKVIHRDLKSRNVVIADDGLKICDFGASRFHNHTTHMSLVGTFPWMAPEVIQS 180
Mus musculus    121 LHMEAPVKVIHRDLKSRNVVIADDGLKICDFGASRFHNHTTHMSLVGTFPWMAPEVIQS 180
Xenopus laevis  121 LHMEAPIKVIHRDLKSRNVVITVDGLKICDFGASRFHSHTTHMSLVGTFPWMAPEVIQS 180

Homo sapiens    181 LPVSETCDTYSYGVVLWEMLTREVPFKGLEGLQVAWLVVEKNERLTIPSSCPRSFAELLH 240
Mus musculus    181 LPVSETCDTYSYGVVLWEMLTREVPFKGLEGLQVAWLVVEKNERLTIPSSCPRSFAELLH 240
Xenopus laevis  181 LPVSETCDTYSYGVVLWEMLTREVPFKGLEGLQVAWLVVEKNERLTIPSSCPRSFAELMH 240

Homo sapiens    241 QCWEADARKRPSFKQIISFLESMSNDTSLPDKCNSFLHNKAEWRCEIEATLERLKRLERD 300
Mus musculus    241 QCWEADARKRPSFKQIISFLESMSNDTNLPDKCNSFLHNKAEWRCEIEATLERLKRLERD 300
Xenopus laevis  241 QCWEADSKRPSFKQILSFLESMSNDSKLPDKCNSFLHNKAEWRCEIEPTLERLKRLERD 300

Homo sapiens    301 LSPKEQELKERERRLKQWEKKLTEQSNTPLLPSFPEGAVTDDEVKCVVQCLVRKGDSSAE 360
Mus musculus    301 LSPKEQELKERERRLKQWEKKLTEQSNTPLLPSFPEGAVTDDEVKFVVQCLVRKGESSVE 360
Xenopus laevis  301 LSYKEQELKERERRLKLWEKKLTEQSNTPLLPSFDECSVTDEIVFVVMQCLVKSDDENI- 359

Homo sapiens    361 TAASNGESHGMNPSLQAMMLNGFGDIPSMNKAGAVWHSGMQINMQAKQNSSKTTGKRGK 420
Mus musculus    361 TAASNGESHGMNPSLQAMMLNGFGDVPSMNKAGAVWHSGMQINMQAKQNSSKTTGKRGK 420
Xenopus laevis  361 TAASNGEVQGMNQSLQAMM-NGFGNIPSMNVVGPVWHSGMQINMQAKQNSSKTTGVRGK 419

Homo sapiens    421 KQNMALGFSDFDLSEGDDDDDDGEEEDNDMDNSE------------ 455
Mus musculus    421 KQNMALGFSDFDLSEG-DDDDHDGDDAENDVDNSE------------ 454
Xenopus laevis  420 KQNMALGFSDFDWSDDSSE------------------------------ 438
```

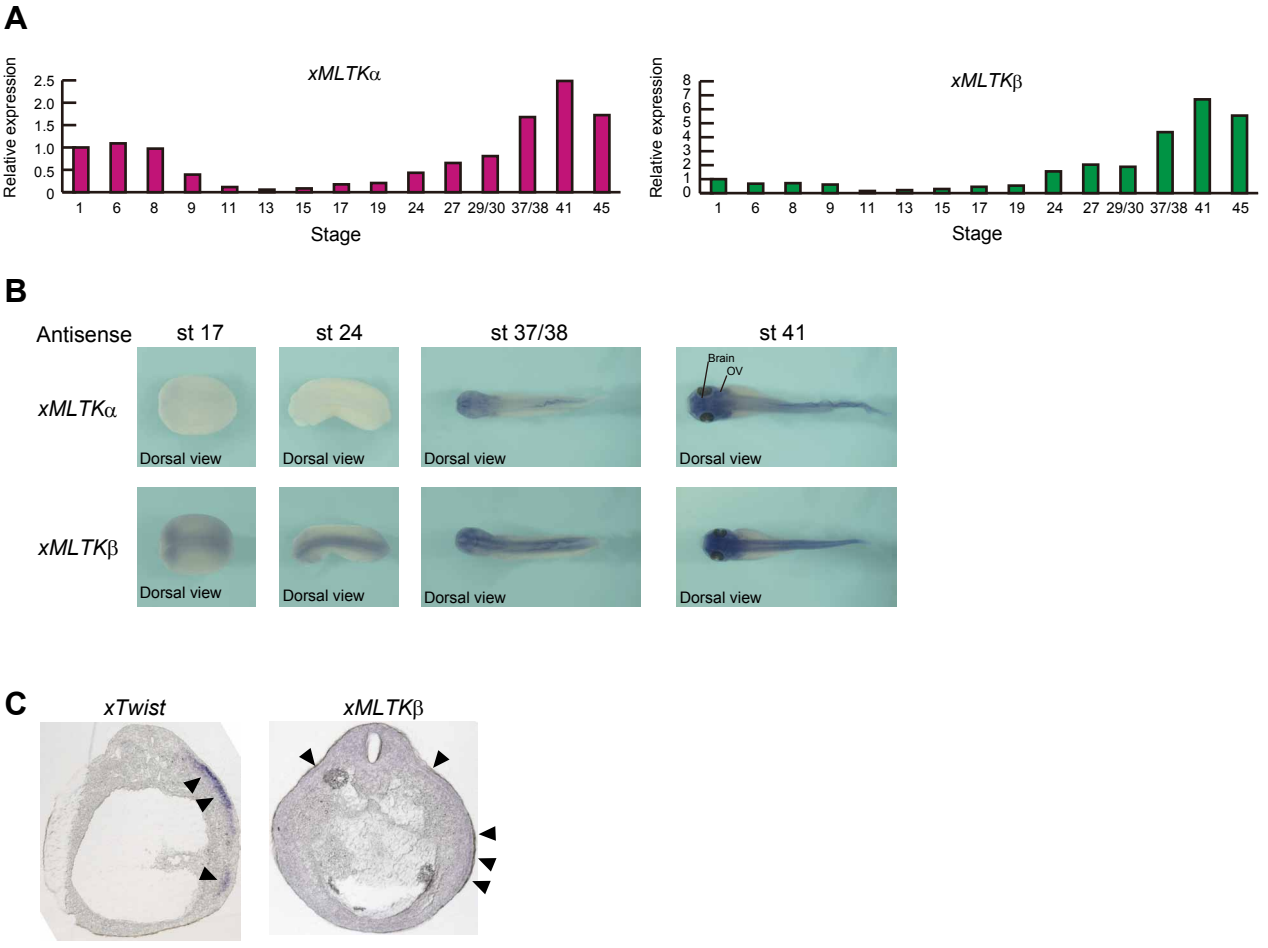
A
xMLTKα
Relative expression
2.5
2.0
1.5
1.0
0.5
0
1 6 8 9 11 13 15 17 19 24 27 29/30 37/38 41 45
Stage
xMLTKβ
Relative expression
8
7
6
5
4
3
2
1
0
1 6 8 9 11 13 15 17 19 24 27 29/30 37/38 41 45
Stage
B
Antisense
st 17
st 24
st 37/38
st 41
xMLTKα
xMLTKβ
Brain
OV
Dorsal view
C
xTwist
xMLTKβ

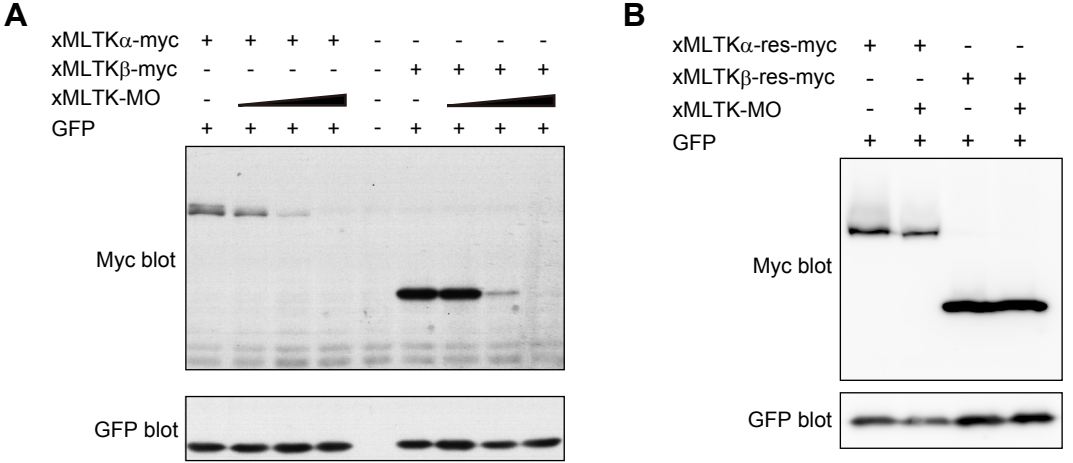
A
xMLTKα-myc + + + + - - - - -
xMLTKβ-myc - - - - - + + + +
xMLTK-MO - - -
GFP + + + + - + + + +
Myc blot
GFP blot
B
xMLTKα-res-myc + + - -
xMLTKβ-res-myc - - + +
xMLTK-MO - + - +
GFP + + + +
Myc blot
GFP blot

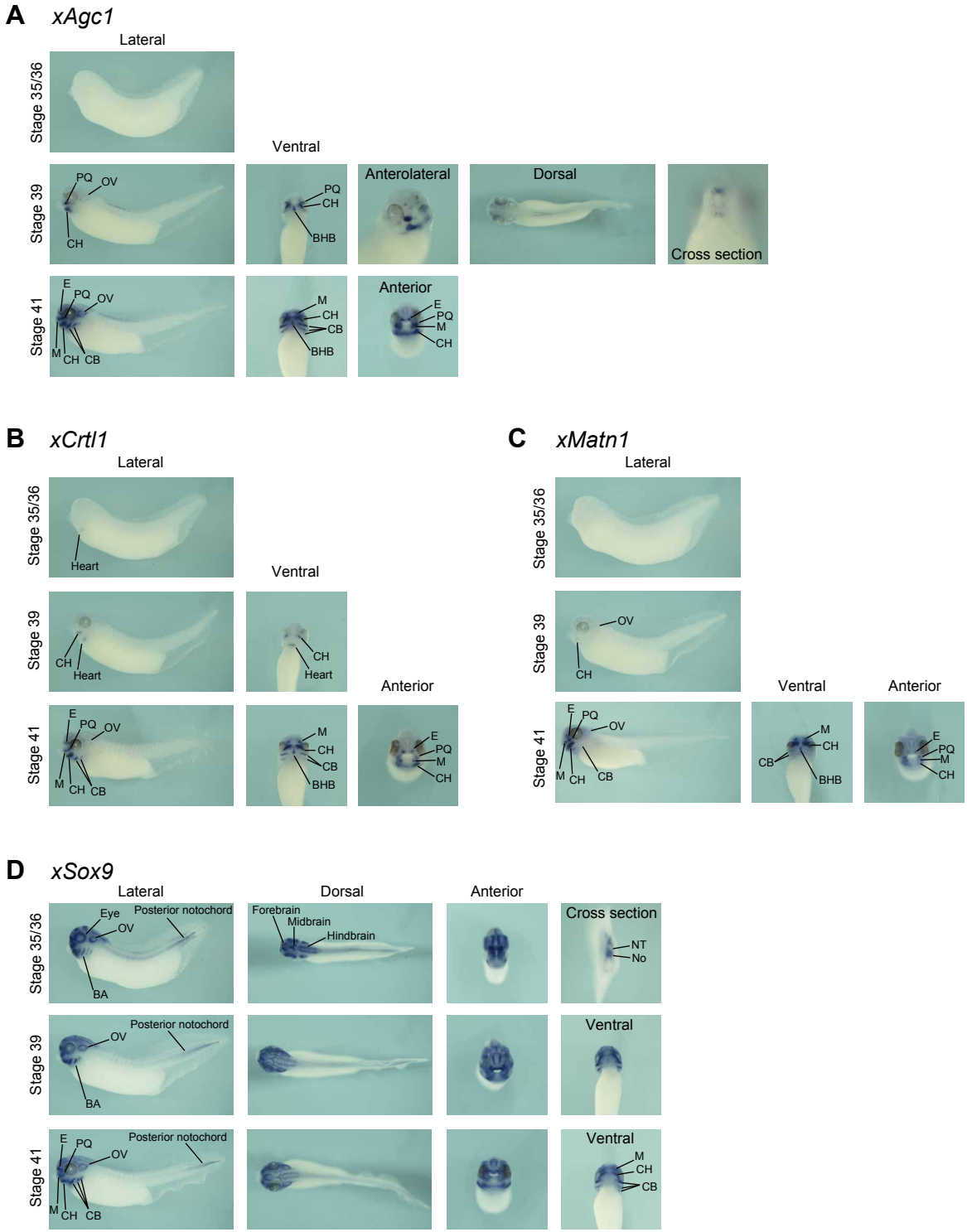
A
xAgc1
Lateral
Ventral
Anterolateral
Dorsal
Cross section
Anterior
Stage 35/36
Stage 39
Stage 41
PQ
OV
CH
BHB
E
M
CB
B
xCrtl1
Heart
C
xMatn1
D
xSox9
Posterior notochord
Eye
BA
Forebrain
Midbrain
Hindbrain
NT
No

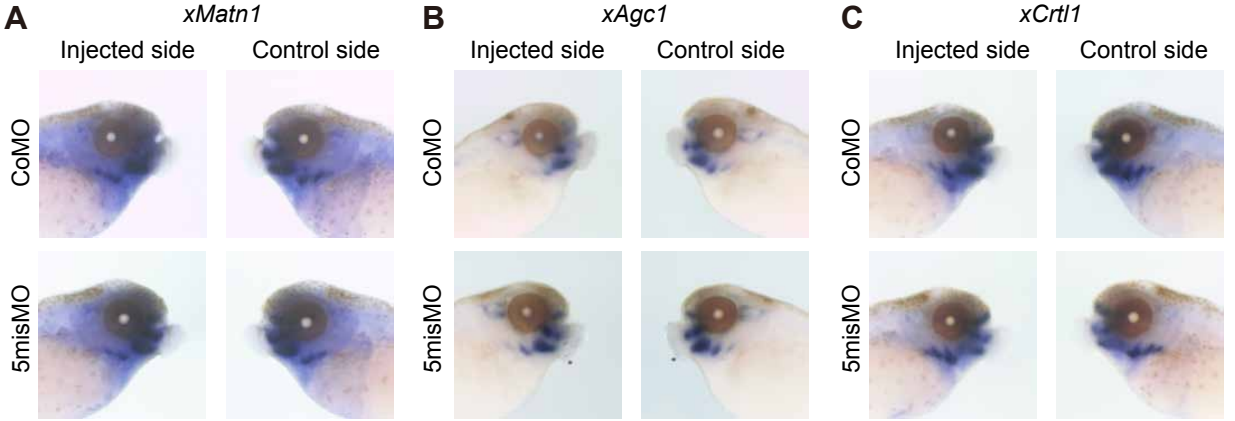
A
xMatn1
Injected side
Control side
CoMO
5misMO
B
xAgc1
Injected side
Control side
CoMO
5misMO
C
xCrtl1
Injected side
Control side
CoMO
5misMO

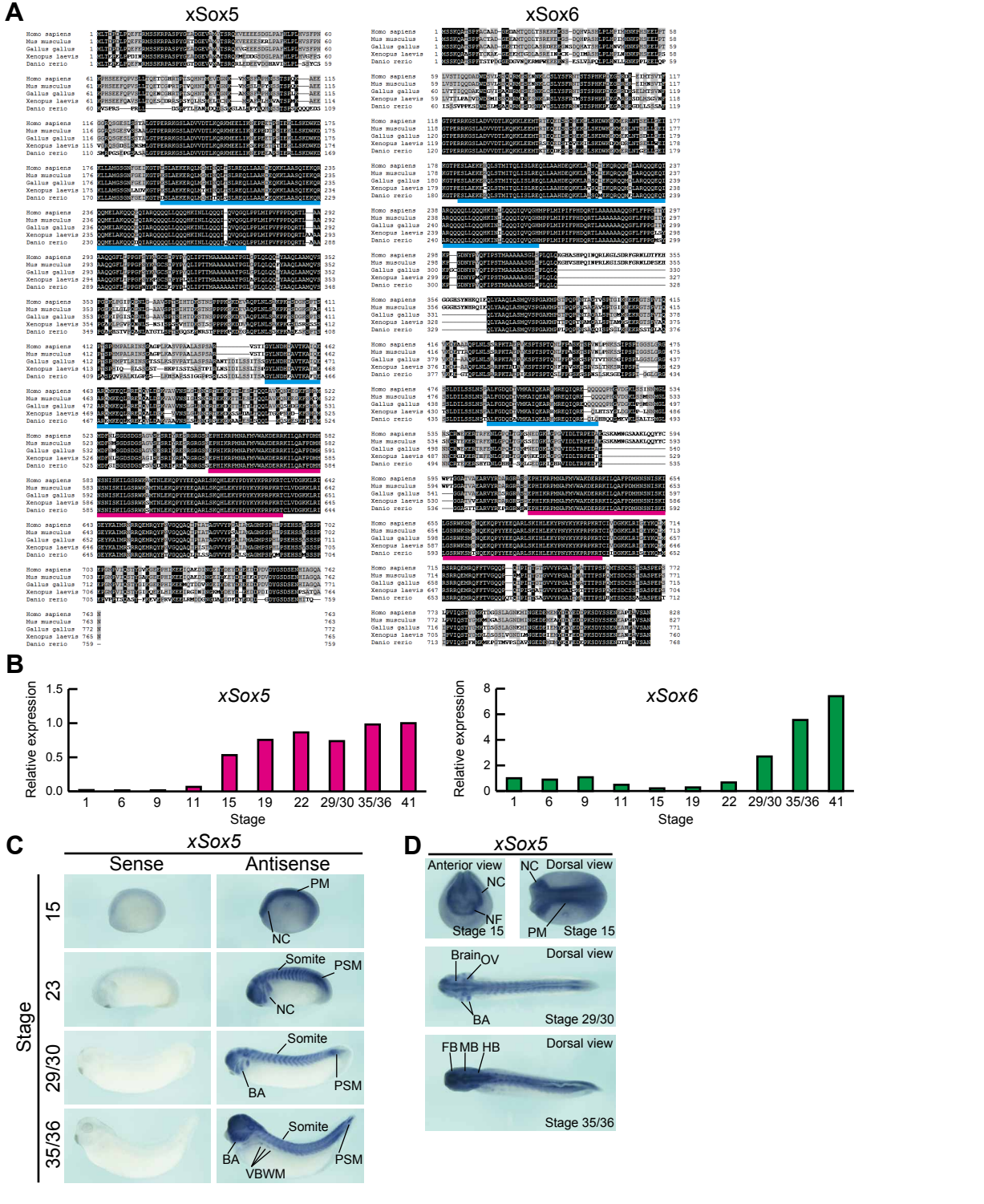
A
xSox5
xSox6
B
xSox5
xSox6
Relative expression
Stage
C
xSox5
Sense
Antisense
Stage
15
23
29/30
35/36
PM
NC
Somite
PSM
BA
VBWM
D
xSox5
Anterior view
Dorsal view
NC
NF
Stage 15
Brain
OV
BA
Stage 29/30
FB
MB
HB
Stage 35/36


A
Uninjected
xSox5-MO
Dorsal view
Lateral view
B
Uninjected
xSox5-MO
xSox6-MO